0044

PUERTO RICO NUCLEAR CENTER

RESONANCE IN RADIATION EFFECTS

Technical Report No. 1

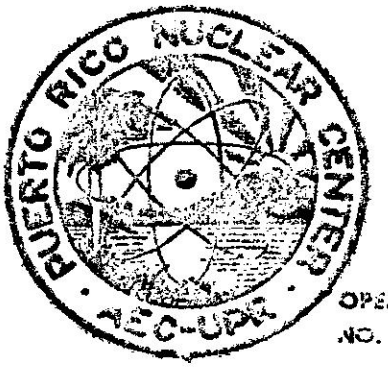

OPERATED BY UNIVERSITY OF PUERTO RICO UNDER CONTRACT
NO. AT (40-1)-1833 FOR U. S. ATOMIC ENERGY COMMISSION

RESONANCE IN RADIATION EFFECTS

I. RESONANCE RADIATION EFFECTS OF LOW ENERGY MONOCHROMATIC X-RAYS ON CATALASE

II. CHARACTERIZATION OF A MONOCHROMATIC HIGH INTENSITY VARIABLE WAVELENGTH X-RAY SOURCE IN THE 5-20 KEV REGION

Henry J. Gomberg, Principal Investigator

Robert A. Luse
Florencio Vázquez Martínez

Progress Report #1

Work performed at Puerto Rico Nuclear Center
Mayaguez, P.R., under U.S. Atomic Energy
Commission Contract AT(40-1)-1833 (Project 14)

January 1963

TABLE OF CONTENTS

Preface 1

Section I. Resonance Radiation Effects of Low Energy Monochromatic X-Rays on Catalase

A. Summary 3

B. Introduction 3

C. Experimental Procedures 4

1. Development of Present Irradiation system 4

2. Development of Ferrous-Ferric Micro-dosimetry System 7

3. Assay for Catalase Activity 10

D. Experimental Results 14

1. Energy Output of X-irradiation System 14

2. Resonance Radiation Effects in Catalase 17

E. Conclusions and Discussion 20

F. Proposals for Future Research 23

G. Appendix 25

1. Notes on Catalase Assay Calculation 25

2. Survey of Radiation Levels About X-irradiation Equipment 30

3. Preliminary Experiments on the Culture of E. coli .. 31

H. Literature References 33

Section II. Characterization of a Monochromatic High Intensity Variable Wavelength X-Ray Source in the 5.20 Kev Region

A. Summary .....

B. Introduction .....

C. General Properties of X-ray Production and Diffraction .

D. Intensity and Energy Distribution .....

E. Characteristics of X-ray Tube .....

F. Analysis for Harmonics in X-ray Beam .....

1. Absorption Method .....

2. Double Diffraction .....

3. Application .....

G. Orientation of X-ray Tube, Protractor, and Soller Slits for Optimum Intensity and Resolution .....

1. Tube Position .....

2. Small Protractor Position .....

3. Use of Soller Slits .....

H. Literature References .....

List of Figures .....

List of Tables .....

PREFACE

H. J. GOMBERG

Reasonably definitive and quantitative results from a new approach to the question: "What is the effect of ionizing radiation on matter?" are now beginning to emerge. This new approach involves study of effects produced by radiation from adjustable monochromatic sources. In general x-radiation effects have been observed to vary slowly as a function of radiation energy. However, little work has been done in the region of x-ray energies below twenty kilovolts, a region of considerable importance since it contains the K-edge absorption energies of the constituent atoms of most living systems. X-radiation of such energies is produced from incident radiation of much higher energies (as Cobalt-60 gamma, 250 Kv x-rays) by degradation through Compton scatter.

It was felt important, therefore, to study x-radiation effects in the 5-20 Kv energy range upon biological systems, which are composed primarily of light elements with but traces of medium atomic weight elements. As a first system for study, the enzyme catalase, containing four atoms of iron in its porphyrin ring structure, was chosen and the question asked: Does radiation absorbed by the iron atom produce more damage (inactivation) per electron volt absorbed than radiation absorbed only by the light elements (carbon, hydrogen, oxygen, etc.), which make up the bulk of the catalase molecule? Experiments were designed to show or disprove the presence of a true action spectrum of radiation damage in the kilovolt region. The presence of such a spectrum indicates unique effects of such radiation, entirely divorced from the general "indirect" effects of radiation (which may be simulated chemically).

A group at the University of Michigan, under the direction of Dr. Henry Gomberg, has been looking into this problem for some time. Two separate studies have been carried out by this group on the enzyme catalase. One was done by Dr. Ardath H. Emmons and another by Mr. Peter Paraskevoudakis. Both demonstrate that 100 electron volts absorbed at photon energies just beyond the K-absorption edge of iron produce substantially more damage than 100 electron volts at energies below the iron K-edge. Damage was measured as reduction of the ability of catalase to react with hydrogen peroxide.

On the other hand, tests made by Dr. William Clendenning in the same group on the free radical yield in 1-bromo-butane, as determined by reaction with DPPH, showed no unique response as a function of energy. Likewise, studies made by Dr. Marvin Atkins on damage through irradiation at the "L"-edge of certain mercury organo-metallic compounds yielded negative results.

Recently, Dr. Gomberg moved to Puerto Rico where a new group, attacking the same problem but with different equipment and under different environmental conditions, was established. The Ann Arbor group is continuing its study under the leadership of Dr. Hoyt Whipple. In Puerto Rico, Dr. Robert Luse has made a completely independent rerun of the catalase experiments and has confirmed the existence of a uniquely high damage rate for photon energies in the vicinity of the K-absorption edge in catalase.

In the course of this work, Dr. Vázquez Martínez, also of the PRNC staff, has developed extremely effective techniques for obtaining substantial yields of monochromatic x-rays for irradiation purposes from a standard General Electric Co. XRD-type spectrometer. Many

incidental, but significant problems have been solved or are being worked on in the course of this research. These include a true micro-calorimeter for low energy x-rays, being developed in Ann Arbor, and high sensitivity chemical dosimetry, being developed in Puerto Rico.

Work is now in progress at PRNC on the x-ray action spectrum of carboxypeptidase (a zinc metallo-enzyme) and on E. coli.

RESONANCE RADIATION EFFECTS OF LOW ENERGY MONOCHROMATIC X-RAYS ON CATALASE

Robert A. Luse

A. SUMMARY

Experiments using monochromatic x-radiation in the energy range 6.4 - 8.3 Kev have shown increased inactivation of the metalloenzyme catalase at or near the K-absorption edge of iron (7.11 Kev). This is taken to confirm the resonance radiation hypothesis of Gomberg and previous experimental work of Emmons and Paraskevoudakis.

X-radiation intensities of 2×10^{11} photons per hour have been measured in the sample holder with Fricke ferrous ammonium sulfate dosimeter. A more sensitive method for detection of the ferric ion produced has been developed, using the ferric-thiocyanate complex.

B. INTRODUCTION

Previous work by Emmons (5) and by Paraskevoudakis (8) has indicated that there is an enhanced inactivation of the metalloenzyme catalase by monochromatic x-rays at wavelengths near the K-absorption edge of iron. Indeed, a plot of enzyme inactivation as a function of the x-radiation wavelength (or photon energy) follows closely the normalized mass absorption spectrum for iron (see Figs. I-1 and I-2). Since no such resonance radiation effects have been reported by other workers, it was desired to confirm the work of Emmons and of Paraskevoudakis using other equipment and personnel. The present report is concerned with such confirmatory experiments.

C. EXPERIMENTAL PROCEDURES

1. Development of present irradiation system.

To obtain x-radiation of precise energy, the irradiation system described in this report by Vázquez Martínez was utilized. Here a portion of the x-ray energy produced in the x-ray tube was selected by collimation and crystal diffraction, so that a beam of monochromatic x-rays having photon energies within the 4-50 Kev range and with a high purity of energy (± 50 ev) was available.

The characteristics of this irradiation beam defined the requirements for the holder in which the enzyme solutions were placed, vis: irradiation chamber dimensions 9mm. wide, and 4 mm. deep; vertical solution height not to exceed 6 mm.[1]

Irradiation of solutions of catalase was carried out in the sample holder sketched in Fig. I-3.[2] This holder is constructed of

---

[1] Measurement of the beam area and position was done by placing a 4 x 4 cm sheet of X-ray film (in light proof envelope) directly in front of the sample holder. After a short irradiation period, the position of the film relative to the holder was marked by piercing envelope, film, and holder with a sharp scribe. After photographic development of the film, it was replaced on the holder, and the holder adjusted to coincide with the darkened area of the film. Later, very accurate characterization of the distribution of energy across the X-ray beam was done by Vázquez (15).

[2] During the course of early work, there were utilized three other sample holders having the characteristics tabulated below. Experience gained in their use allowed design of the present holder.

Cell	Construction	Capacity	Solution thickness
A	round polyethylene bottle top	1.5 ml	9 mm
B	jacketed lucite block	1.0	16
C	lucite block with small compartments ("Michigan cell")	0.2	2

Cells A and B had Mylar windows, cell C was covered with scotch tape until it was found that contact with such tape caused inactivation of catalase solutions.

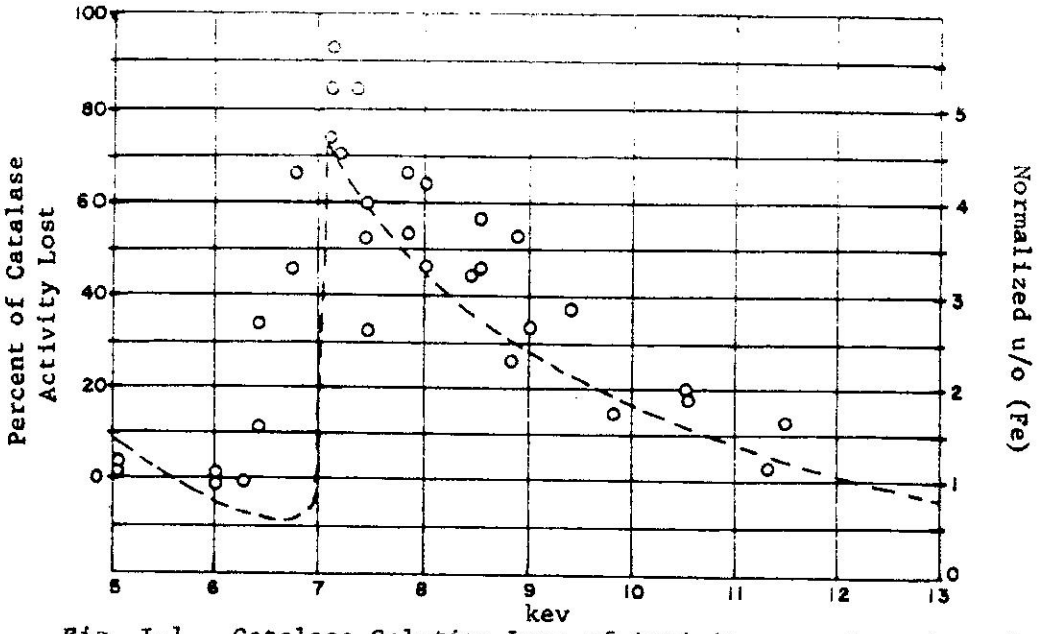

Fig. I-1. Catalase Solution Loss of Activity as a Function of X-ray Energy. Data of Emmons, Ref. 1,2. Normalized iron-mass absorption curve is given by the brocken curve.

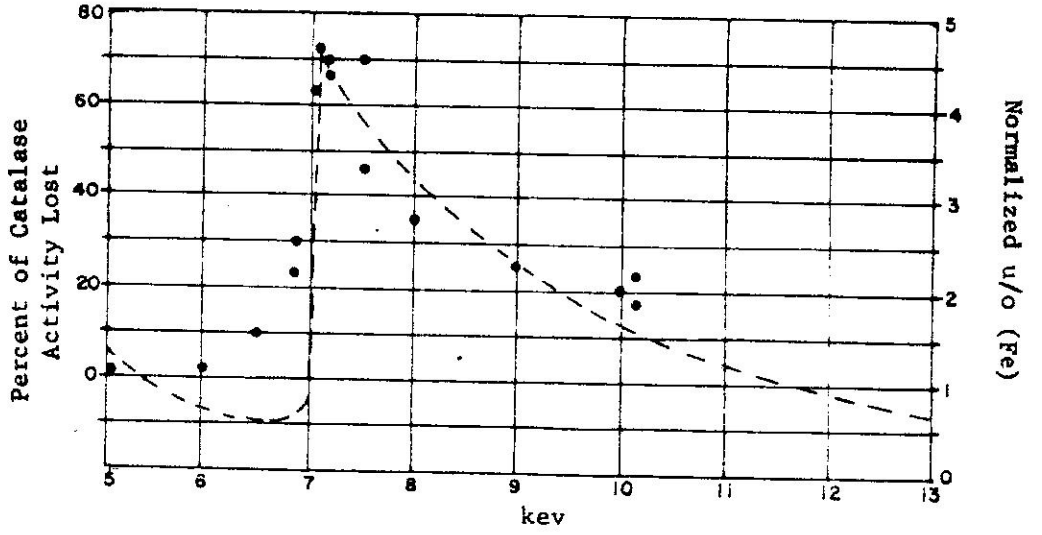

Fig. I-2. Refer to caption above. Data of Paraskevoudakis.

Note: For Fig. I-1, each sample absorbed a dose of 1.8×10^{12} and for Fig. I-2, 1.2×10^{13} X-rays/cm^3. The incident dose rate was 9.5×10^{10} X-rays/cm^3-hr. for Fig. I-1. For Fig. I-2 th dose rate increased from 1.5×10^{11} at 5 kev to 7.0×10^{11} X-rays/cm^3-hr at 10 kev.

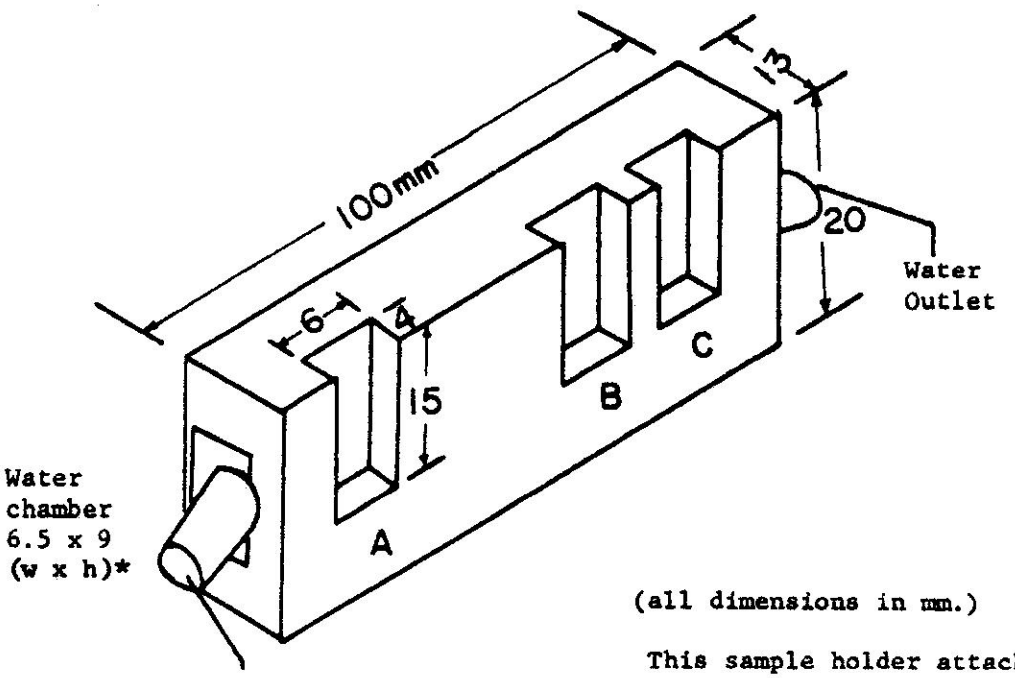

(all dimensions in mm.)

This sample holder attached to lucite sheet 100 x 70 x 1.5, which is bolted in place on detector housing

* Distance between chamber and sample compartments - 2.5

Fig. I-3. Sketch of sample holder

methacrylate plastic (Lucite) with a 0.002 inch thick Du Pont Mylar polyester film attached to its face; these materials are relatively transparent to low-energy x-rays and are non-reactive chemically with the biological sample. Compartment thickness was determined by balancing the factors of solution absorption and sample size: a 2 mm. sample thickness was measured to absorb approximately 95% of incident 7 Kev photons, yet this thickness would permit only a 100 µl sample, too small for accurate manipulation and analysis. A depth of 4 mm. permitted a 220 µl. sample, and masking of solution under such conditions of complete absorption was avoided by mechanical stirring with a 0.5 mm. glass rod inserted into the solution and rotated at 88 rpm. To minimize evaportation and inactivation of the catalase solution, samples were covered and maintained at 5°C. by passing water from a constant temperature refrigerated bath through the holder block.

2. Development of ferrous-ferric micro-dosimetry system.

The prime requirement specified for the dosimeter system was the ability of direct substitution for the sample, so that values of radiation intensity measured with the dosimeter correspond directly with those absorbed by the biological sample. Other considerations were simplicity of use and reliability in the low dose ranges involved in this work.

The Fricke ferrous-ferric dosimeter is the most commonly used and best characterized "secondary standard" available.[1] This dosimeter relies on the oxidation by ionizing radiation of ferrous ion to ferric ion, and determination of the concentration of ferric ion formed by

---

[1] as compared with primary standards such as colorimetry of Hart (7)

its light absorption at 304 mμ (cf. Schuler and Allen,12).Application of this dosimeter is primarily limited by the methods for ferric ion analysis. Recent work by Scharf and Lee (11) has shown that a more sensitive assay for ferric ions is measurement of the absorbance at 224 mμ; here the molar absorptivity[2] of ferric ion is 4565 liter $mole^{-1}$ cm^{-1} compared to the value 2196 at 304 mμ wavelength. That the absorption spectrum for the ferric ammonium sulfate solution used in this work coincides with that of the ferric sulfate solution used by Scharf and Lee was confirmed by laboratory measurement.

A considerably more sensitive assay of ferric ion concentration is measurement of the absorbance of the red-orange ferric-thiocyanate complex; the molar absorptivity of this complex is 10,000 - 14,000 liter $mole^{-1}$ cm^{-1} at 480 mμ (see Fig. I-4). Pribicevic, Gal, and Draganic (10) have characterized this complex formation and proposed its use as a dosimetry system in the 300 - 100 rad dose range. Not all their results could be confirmed, so that further characterization and modification of the system were undertaken. Differences were found in the location of the absorption maximum (480 mμ, not 470 mμ) and in the potassium thiocyanate concentration yielding greatest complex-absorbance (2.0 N, not 0.69 N); these changes were incorporated into the procedure developed. In addition, to avoid dilution of the irradiated solution, optical measurements were taken with the Beckman DU spectrophotometer in cuvettes of 3 mm x 10 mm x 25 mm chamber dimensions; as little as 0.22 ml of solution may be assayed in such cuvettes.

---

[2] The term molar absorptivity is equivalent to the older terms molar extinction coefficient and molar absorption coefficient. This follows the preferred usage of the editors of Analytical Chemistry (1).

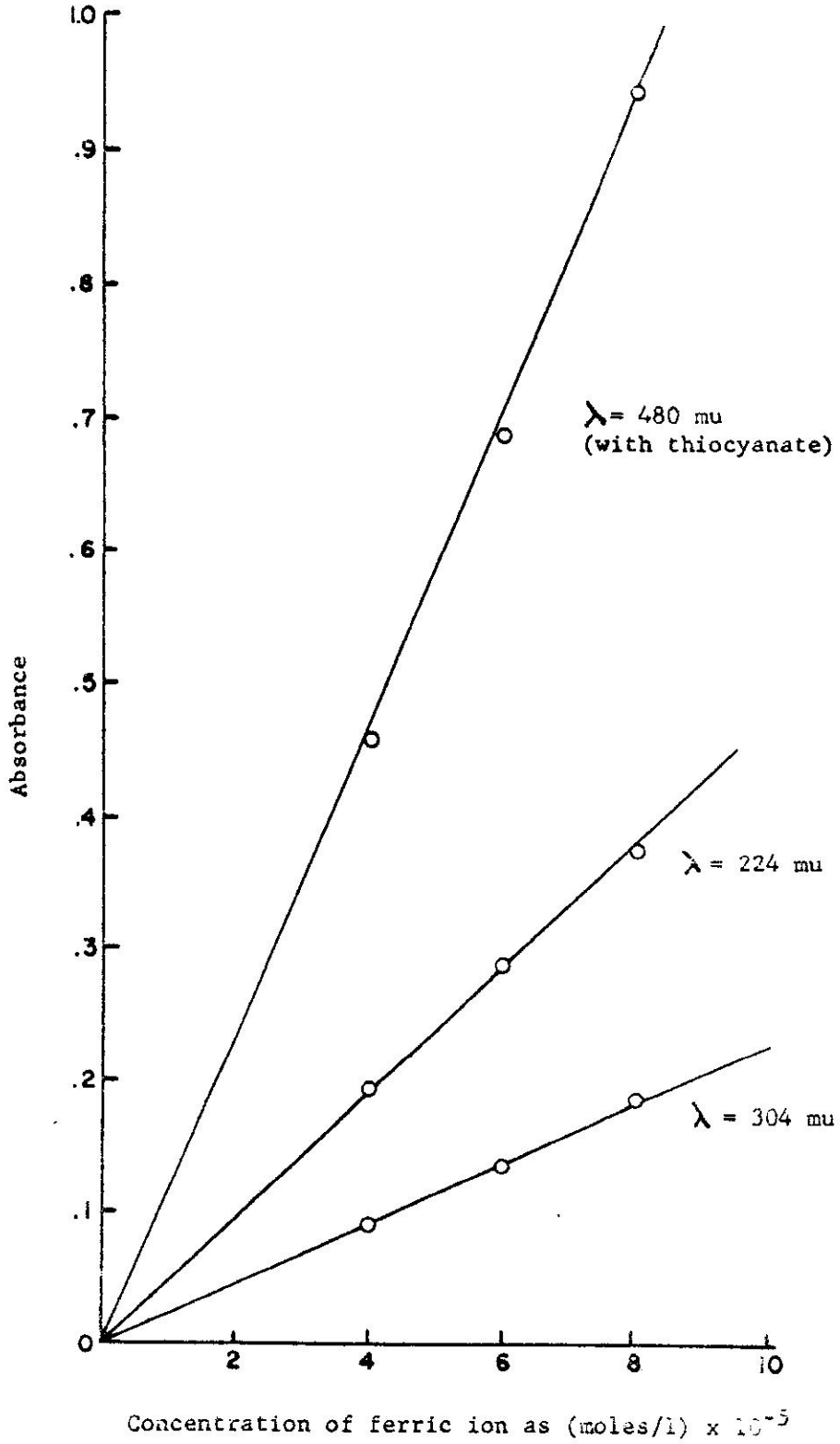

Fig. I-4 Comparison of sensitivity of various methods for determining ferric ion in dosimeter

The procedure for assay of irradiated ferrous dosimeter was as follows: To the four microcuvettes were added portions (approximately 0.23 ml in volume) of 5×10^{-3} M ferrous ammonium sulfate in 0.8 N sulfuric acid, treated vis: a) not irradiated, stored in refrigerator, b) irradiated for the specified time at 5°C. with mechanical stirring, c) and d) controls 1 and 2, kept in holder compartments B and C during irradiation. Measurements of absorbance at 224 and 304 mμ were made, using the stored control as blank. One of the controls was then set aside and 220 μl. of the ferrous solution containing ferric ammonium sulfate to the extent of 1×10^{-5} M ferric ion was placed in this cuvette. Fifty mg. portions of potassium thiocyanate were then added to each cell and dissolved by shaking. Absorbance at 480 mμ was measured after 10 min. The value of the molar absorptivity was calculated from the standard ferric solution and used to estimate the ferric ion concentration in the irradiated and control samples.

3. Assay for catalase activity.

Catalase concentrations were determined using essentially the standard assay developed by Beers and Sizer (2), in which the disappearance of hydrogen peroxide is followed spectrophotometrically at 212 mμ.[1] Catalase activity was expressed in units of enzyme (U) per

---

[1] These authors used 240 mμ wavelength for measurement but show that any wavelength in the 200 - 300 mμ region is appropriate. The 212 mu wavelength was used for two reasons: to repeat work of Emmons and Paraskevoudakis, and to utilize the larger (by nearly five times) molar absorptivity of hydrogen peroxide at the lower wavelength.

mg. of protein, where one unit is equal to that amount of enzyme which will catalyze the decomposition of 1 micromole of hydrogen peroxide per minute under specified conditions.[1]

Assay reagents were as follows: Enzyme solution - An approximately 4.5 mg % solution of catalase (Worthington Biochemical Co. lyophilized material, lot no. CTL 5536) was prepared in 0.067 M potassium phosphate buffer, pH 6.80 (made from 0.067 M solutions of $NaH_2PO_4.H_2O$ and $Na_3PO_4.12H_2O$). Such solutions were stored at 5°C. in red "low actinic" volumetric flasks. Calculation of enzyme concentration by spectrophotometric measurement was done using the molar absorptivity value 340 cm^{-1} mM^{-1} at 405 mμ for horse liver catalase.[2] Substrate solution - A 0.03% (8.8×10^{-3}M) solution of hydrogen peroxide was prepared from Fisher reagent grade 30% material by 1:1000 dilution with 0.067 M phosphate buffer, pH 6.80. This solution was prepared fresh daily before use, as dilute peroxide solutions are not stable at room temperature. Water used for enzyme and substrate solutions was distilled in glass from previously demineralized water. Buffers and water were stored in polyethylene bottles to minimize trace metal contamination.

---

1 Such terminology follows recommendations made by the Commission on Enzymes of the International Union of Biochemistry (see Thompson, 13).

2 Such a calculation indicated that a 4.80 mg. % solution, nominally 2.1×10^{-7} M (molecular weight of 225,000) was actually 1.0×10^{-7} M. This means that the lyophilized material has regained moisture to approximately half its total weight.

The assay procedure was as follows: The sample of catalase solution (normally 0.1 - 0.2 ml. in volume) was placed in a spectrophotometer cuvette (1.0 cm. path length, 4 ml. capacity, fused silica for ultraviolet transmission). At zero reaction time, 2 ml. of substrate was rapidly pipetted into the cuvette, and the change in percent transmittance at 212 mu of the solution measured over the first 90 sec. of reaction time. This change in transmittance was measured using a Servo/riter strip chart recorder attached to the Beckman DU spectrophotometer with a Beckman energy recording attachment (ERA). The limits of pen travel on the chart were defined prior to this measurement by adjusting the pen to 0% transmittance with the spectrophotometer dark current adjust with no light striking the photocell, and then to 100% transmittance with the ERA "100% adjust" knob with light passing through a solution of buffer only. No attempt was made to add the hydrogen peroxide to the enzyme and to start the recorder simultaneously; the substrate was added at zero time (as judged from a sweep second hand timer), the spectrophotometer shutter was opened, and the recorder was started, in a sequence requiring about seven sec. The ninety second interval was accurately measured, at which point the shutter was closed causing a rapid deflection of the chart pen to zero. Points on the chart corresponding to 60 sec. were determined by carefully measuring back from this deflection point with a ruler. Since chart speed was 18.3 cm. $min.^{-1}$, the 60-90 sec. interval was equivalent to 9.15 cm. In some measurements, increased sensitivity in the chart recording was achieved by setting the 100% T margin with a solution of measured absorbance approximately 0.9. By this method, absorbances in the 0.9 - 2 region were more accurately measured, and the slope of the curve %T vs. time increased by a factor of approximately eight.

The values of %T taken from the chart strip recording were converted to absorbance values by the relationship

$$\text{absorbance} = \log (100/\text{percent transmittance} \qquad \text{(eqtn. 1)}$$

and these absorbance values used in the equation

$$\text{enzyme units per mg.} = \frac{\Delta A \text{ per minute} \times 1000}{146 \times \text{mg. catalase per ml. of reaction mixture}} \qquad \text{(eqtn. 2)}$$

where 146 is the molar absorptivity of hydrogen peroxide at 212 mμ (measured in this laboratory).[1]

---

[1] at the same time that the molar absorptivity at 240 mμ was measured and found to agree with published values.

D. EXPERIMENTAL RESULTS

1. Energy output of x-irradiation system

The intensity of x-radiation in the 6.5 - 7.5 Kev photon energy range, as measured by the ferrous dosimeter, is shown in Fig. I-5, based on data listed in Table 1.

The following equations were used in calculating this data:

$$\left\{\begin{matrix}\text{Amount of ferric ion} \\ \text{in sample, as moles/ml}\end{matrix}\right\} = \frac{\left(\begin{matrix}\text{absorbance of sample corrected for} \\ \text{blank at } \lambda \text{ of measurement}\end{matrix}\right)}{\left(\begin{matrix}\text{molar absorptivity of ferric ion} \\ \text{at } \lambda \text{ of measurement}\end{matrix}\right)} \times 10^{-3}$$

$$\text{or, } C = A/1000\varepsilon \qquad \text{(eqtn. 3)}$$

Molar absorptivity of ferric ion at 224 and 304 mμ is 2196 and 4565 liter $mole^{-1}$ cm^{-1} respectively at 25°C. The molar absorptivity of the thiocyanate complex at 480 mμ was estimated from ferric standards, as described previously.

$$\left\{\begin{matrix}\text{the rate of radiation absorption} \\ \text{by the sample, in ergs } ml^{-1} \text{ } hr^{-1}\end{matrix}\right\} = I = \frac{C \cdot f \cdot 6.02 \times 10^{23}}{Y \cdot t} \qquad \text{(eqtn. 4a)}$$

where C = concentration of ferric ion, moles/ml.

f = factor for conversion of electron volts to ergs, 1.6×10^{-12} erg/ev

Y = the ferrous ion yield (G value), equal to 0.135 ions oxidized per electron volt, in the 8 - 10 Kev range (Cottin and La Forte, 4)

t = period of irradiation, in hours

$$\text{or, I (as ergs } ml^{-1} \text{ } hr^{-1}) = \frac{C}{t} \cdot 7.14 \times 10^{12} \qquad \text{(eqtn. 4b)}$$

I, furthermore, as photons ml^{-1} hr^{-1} = $\frac{C}{t} \frac{1}{\text{E per photon, in ev}} \cdot \frac{1}{1.6 \times 10^{-12}}$ (eqtn. 5a)

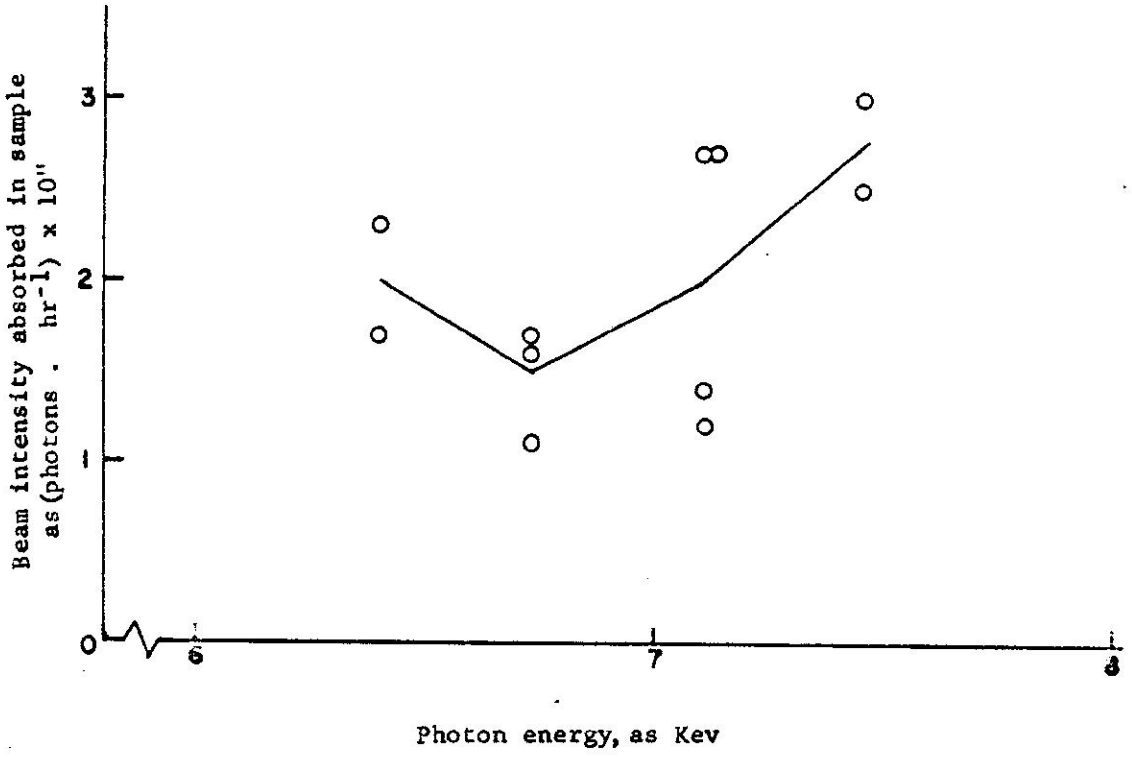

Fig. I-5. Monochromatic x-ray beam intensity as function of photon energy

TABLE 1. MEASUREMENT OF MONOCHROMATIC X-RAY BEAM INTENSITY, USING FERROUS DOSIMETER

Date	2θ (Li F crystal)	E mv^{-1}, as Kev	Irrn. period in hrs.	λ of measmt.	Absorbance of soln. in compartment A	B	C	ΔA*	ε**	C, as (moles ml^{-1}) x 10^{-9}	I, as (ergs ml^{-1} hr^{-1}) x 10^{3}	I, as (mv. ml^{-1} hr^{-1}) x 10^{11}	I', as (hv. hr^{-1}) x 10^{11}
11/14/62	51.2°	7.11	6.0	304	.035	.016	.018	.019	2200	8.6	10.2_0	9.0	2.7
				224	.056	.028	.033	.028	4570	6.1	7.2	7.1	1.7
11/28/62	57.5	6.40	6.0	304	.027	.009	.017	.018	2215	8.1	9.6	9.4	2.3
				224	.055	.025	.054	.030	4570	6.6	7.8	6.9	1.4
11/29/62	51.2	7.11	6.0	304	.021	.008	.020	.013	2215	5.9	7.0	6.2	1.2
12/17/62	51.2	7.11	7.5	224	.124	.066	.061	.063	4590	13.7_0	13.0_0	10.9	2.7
				224	.045	.022	.053	.023	1570	5.0	7.1	6.6	1.6
12/18/62	54.5	6.73	5.0	304	.020	.008	.029	.012	2240	5.3	7.6	7.0	1.7
				224	.058	.027	.000	.058	4570	12.7	14.0_0	11.7	3.0
1/3/63	49.0	7.43	6.5	304	.024	.009	.000	.024	2240	10.7	11.8	9.9	2.5
1/8/63	54.3	6.73	10.0	304	.024	.014	.010	.014	2200	6.4	4.6	4.2	1.1

* $\Delta A = A_A - (A_B \text{ or } A_C)$, whichever is smaller.

** Molar absorptivity values were corrected for temperature using data of Scharf and Lee (11).

$$= \frac{C}{t} \cdot \frac{4.46 \times 10^{24}}{G \ \mu v^{-1}} \qquad \text{(eqtn. 5b)}$$

I, as photons. hr^{-1} absorbed in sample

$$= I' = (I, \text{ as photons} \cdot ml^{-1} \ hr^{-1}) \times (\text{sample volume in ml.}) \qquad \text{(eqtn. 6)}$$

$$\text{Total dose delivered to sample} = I' \cdot t \qquad \text{(eqtn. 7)}$$

The most important features of these data are a) that the beam intensity is approximately 2×10^{11} photons per hour in the 6.4 - 7.2 Kev photon energy region, b) that the intensity is increasing with increasing photon energy (as found by Paraskevoudakis), and c) that there is no resonance radiation effect in the ferrous dosimeter at the K-absorption edge of iron. This last finding is as expected, since the radiation effect measured is an oxidation, the G value for which is energy independent over at least one hundred orders of magnitude.

2. Resonance radiation effects in catalase

The extent of catalase inactivation by monochromatic x-radiation is shown graphically in Fig. I-6.[1] This curve is based only on most recent data, from experiments in which inactivation of control catalase solutions by scatter radiation was minimized by additional shielding (Table 2). That there is enhancement of catalase inactivation by radiation of energies at or near the K_{α} and K-absorption edges of iron is obvious, and confirms the findings of Emmons and Paraskevoudakis. In general, the shape of the curve approximates that of the iron-mass absorption curve.

---

[1] Vertical arms from these points indicate the extent of difference in duplicate assays on irradiated sample. Horizontal arms indicate the variation in photon energies within the x-ray beam ($\pm$ 50 electron volts).

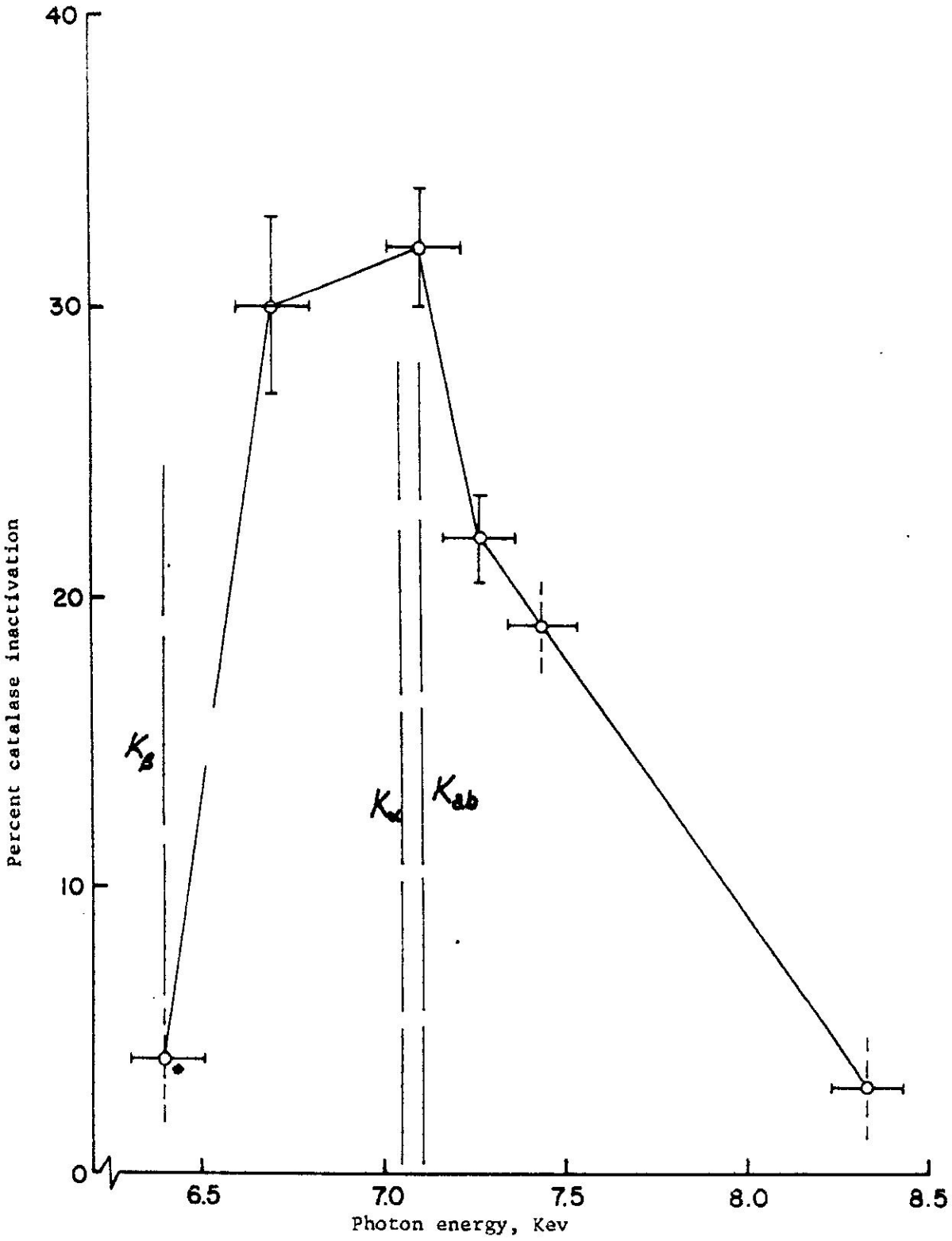

Fig. I-6. Resonance radiation effect of monochromatic x-rays on catalase

Total dose absorbed by sample = 1.4×10^{13} photons (except for starred point, where dose = 0.2×10^{13}

TABLE 2. CATALASE INACTIVATION BY MONOCHROMATIC X-RADIATION

Assay Date	2θ Li F Crystal	E hv^{-1} as Kev	Irrn. period in hrs.	Enzyme activity, as % of stored control			% relative activity of irrad. sample (controls = 100%)	% inactivation by irradiation
				Control (B)	Control (C)	Irrad. (A)		
11/29/62	57.5°	6.40	12	91	96	90	96	4
12/6/62	54.5	6.73	72	96,87	85,81	63,58	70±3	30±3
12/3/62	51.2	7.11	72	90,95	86	64,60	69±2	31
12/10/62	50.1	7.28	72	84,79	84,94	65,67	78±1	22±1
12/13/62	49.0	7.43	72	78,77	98,83	68	81	19
12/17/62	45.0	8.33	75.5	88,102	83,98	90	97	3

E. CONCLUSIONS AND DISCUSSION

It is interesting to compare present dose rates and total doses with those of Emmons and Paraskevoudakis. A summary of these data is given in Table 3. Emmons reports dose rates which are 0.1 to 0.025 those found in this work, and total doses which are 0.02-0.03 present

TABLE 3. SUMMARY OF DOSE RATES AND TOTAL DOSES ABSORBED IN CATALASE SAMPLES

Investigator	Dose rate, as hv hr^{-1}	total dose, as photons	sample volume in ml
Emmons - mixed order	1.7×10^{10}	3.3×10^{11}	0.18
Emmons - first order	4.5×10^{9}	to 5×10^{11}	0.18 or 1.95?
Paraskevoudakis-mixed	$(2.7\text{-}13) \times 10^{10}$	2.2×10^{12}	0.18
Luse - first order	2×10^{11}	1.4×10^{13}	.23
Vázquez - first order (by SPG-1 detector)	1.7×10^{9}	--	--

values. That the extent of catalase inactivation obtained is similar (30-40%) for both studies using first order radiation casts some doubt on the former dosimetry. Emmons found that the intensity of x-radiation (or energy flux) as measured by the SPG-1 detector was about ten percent that measured with the Fricke dosimeter. Comparison of the dose rate values measured by Luse with the Fricke dosimeter and by Vázquez with a similar electronic detector shows that in the present work the counter efficiency is approximately one percent, that is, the counter registers one out of every 100 incident counts. A possible reason for the ten-fold difference is that the surface area of Emmons' dosimeter was not matched to the x-ray beam area, so that the apparent energy flux per cm^2 was in error. For example, it seems that Emmons used a sample holder in his dosimetry studies having a surface area equal to 2.28 cm^2, whereas

the beam area may have been only about 0.24 cm^2. (Possible dimensions, as defined by the collimating slits used, are 0.8 x 0.3 cm.) In the present work, this discrepancy is eliminated since the sample surface exposed to the x-ray beam is exactly the same as the beam area. In simplified form, the scheme below illustrates this situation.

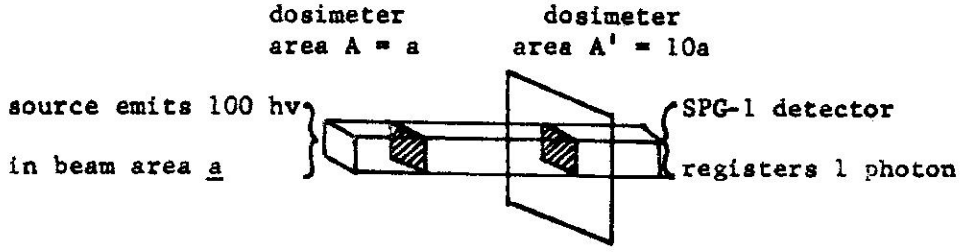

in case 1, dosimeter absorbs 100 hv/A = 100/a; counter efficiency = 1/100

in case 2, dosimeter absorbs 100 hv/A' = 10 hv/a; apparent counter efficiency = 1/10

An apparent quantum yield for catalase inactivation at the K-absorption edge of iron may be calculated from present experimental results, vis:

Quantum yield = molecules inactivated / photons absorbed, where

molecules of catalase inactivated =

$(1 \times 10^{-7}$ moles/l)x(0.25/1000 liters)x(1/3 inactivation)x(6.02×10^{23})

photons of 7.11 kev energy absorbed =

$(2 \times 10^{11}$ hv/hr) x 72 hrs.

Hence the apparent quantum yield =

(5×10^{12}) / (1.4×10^{13}), or 0.36 molecules/photon.[1]

---

[1] The quantum yield calculated is 200-fold less than the 70 molecules inactivated per photon reported by Emmons using dry catalase. Quantum yields considerably greater than unity have not been reported for enzymes in the many studies of non-resonance radiation effects. A part of this discrepancy may be due to error in estimation of doses absorbed in sample.

It must be realized that this apparent quantum yield is not the same as the true quantum yield, since the above is not corrected for absorption by the solvent. An estimate of the relative absorption of 7 Kev photons by solvent and solute in a 1×10^{-7} M catalase solution may be made as follows (cf. data of Emmons):

Material	Total Absorption Coefficient, cm^2/g.	Concentration, g/l.	Mass Absorption, cm^2/l.
Catalase	11.16	0.022	0.24
Water (0.11H, $.890_2$)	0.057 + 13.6= 13.7	1000	13,700

Hence the catalase absorbs 1/57,000 the energy absorbed by the solution.

An exact measure of the quantum yield can be obtained only from experiments using dry enzyme preparations. However, rough estimates may possibly be made by extrapolation from a series of enzyme concentrations.

Calculation also may be made of the G value for catalase based on present results. Since 0.36 molecules are inactivated per photon of 7100 ev energy absorbed by the solution the G value equals 0.005 molecules/100 ev. This is approximately half the value of 0.009 previously reported for x-radiation of much higher energies where the resonant effect is not present.

F. PROPOSALS FOR FUTURE RESEARCH

As present results confirm the presence of a resonant effect in the x-ray inactivation of catalase, it is proposed to enter the second phase of the research--examination of a second metalloenzyme.[1] Carboxypeptidase A has been chosen for study for several reasons, vis:

a) its radiosensitivity should allow much shorter irradiation periods so that use of the present low-intensity x-ray source is feasible;

b) its physical chemical characterization has been well developed by Vallee and coworkers (3, 14), so that it provides a rather well defined enzyme for study;

c) it is presently unique in that the single zinc atom present per molecule which is necessary for peptidase and esterase activity may be replaced with mercury, cadmium, lead, cobalt, nickel, or manganese to give a series of new metallocarboxypeptidases displaying specific activities towards a series of new substrates, characteristic of the particular metal which is incorporated.

This ability of substitution of the metal atom associated with the active site of carboxypeptidase permits the following experiment:

Irradiation with monochromatic x-rays of carboxypeptidases containing different metals, e.g. zinc and nickel, at the K-absorption edges of the respective metals. Enhanced inactivation of the zinc-enzyme would be expected at 9.66 Kev (zinc K_{ab}), inactivation of the

---

[1] Irradiation of catalase at higher doses would best wait until a more intense x-ray source is available.

nickel enzyme at 8.33 Kev (nickel K_{ab}); no inactivation should be produced in the zinc enzyme by photons of 8.33 Kev, nor in the nickel enzyme by photons of 9.66 Kev energy.

Phase three of the experimental program will be a study of living systems where the resonance effect may be observed. Here the single-celled bacterium Escherichia coli provides a well-characterized test organism. In addition, it contains the zinc metalloenzyme alkaline phosphatase, which is obtainable in pure form (9). It is proposed to compare the resonance radiation effect in this enzyme (inactivation vs. photon energy) with the resonance radiation effect in the bacterium (percent survival vs. photon energy). Should the enzyme be essential for bacterial reproduction, the two effects should be similar.[1]

A whole new range of experiments can be initiated when vacuum x-ray equipment becomes available. With photons of 2.1 and 2.5 Kev energies, the resonance radiation effects may be studied in sulfur and phosphorus atoms respectively. At this point, the importance of disulfide bonds to three-dimensional enzyme structure and the role of inorganic phosphate atoms in the active site of certain enzymes (e.g., alkaline phosphatase) may be studied.

It is hoped that such resonance radiation studies will introduce a new dimension of specificity in the field of radiobiology. Low energy monochromatic x-radiation offers a tool as "clean" as monochromatic ultraviolet light, but in an energy range one to three thousand-fold that of UV. With such a tool, a host of new radiobiological studies in the important field of enzyme structure and function becomes possible.

---

[1] It is interesting to speculate on enzyme-nucleic acid interrelations at this point.

G. APPENDIX

1. Notes on catalase assay calculation

The method of calculating catalase activity given in this report differs from that used by Emmons (and presumably, Paraskevoudakis), who made use of the following relationships:

$$K_1 = \frac{\log_e}{t} \frac{(100 - T_1)}{(100 - T_o)} \qquad \text{(eqtn. 1)}$$

and $K_1 = 1.2 \times 10^{-3} \text{ (concentration)}^{0.8}$ (eqtn. 2)

K_1 was determined in each assay by plotting the percent transmittance values measured by the recording system as log (100 - T) and determining the slope of this line over the first 60 sec. of enzyme reaction, vis:

$$m = \frac{\Delta y}{\Delta x} = \frac{\log (100 - T_1) - \log (100 - T_o)}{60 \text{ sec.}} = \frac{\log}{60} \frac{(100 - T_1)}{(100 - T_o)}$$

(eqtn. 3)

That values so calculated are negative seems unrecognized by Emmons. An empirical linear relationship was found between log K_1 and log enzyme concentration in the 0.3 - 2 x 10^{-7} M range. The equation best fitting this line (eqtn. 2) was used subsequently to estimate enzyme concentration in controls and irradiated samples.

This method was rejected because it is not an accurate expression of the fundamental kinetics of the enzyme reaction. The reaction of catalase with hydrogen peroxide is described by first order kinetics during the initial part of the reaction (before product concentration reaches a point where the enzyme is poisoned. The equations describing such first order reactions are

$K_1 = \frac{1}{t} \log_e (S_o/S_1)$ where S_o and S_1 = substrate concentrations at time 0 and time 1

(eqtn. 4)

and $K_1 = k$ (enzyme concentration) (eqtn. 5)

Beers and Sizer (2) have shown that 0.01 - 0.02 M hydrogen peroxide substrate follows Beer's Law for wavelengths of 210 - 300 mμ, i.e. absorbance, A, is proportional to S, hence

$$K_1 = \frac{1}{t} \log_e (A_o/A_1). \quad \text{(eqtn. 6)}$$

Substitution of percent transmittance for absorbance results in an equation of the form

$$K_1 = \frac{\log_e}{t} \frac{(-\log (To/100)}{(-\log (T_1/100)} = \frac{\log_e}{t} \frac{(\log 100 - \log T_o)}{(\log 100 - \log T_1)} . \quad \text{(eqtn. 7)}$$

(The term (log 100 - log T) is not equal to log (100 - T). E.g. if T = 22%, log 100 - log T = 0.658; log (100 - T) = 0.892).

Comparison of the shapes of the curves obtained by plotting equations 1 and 5 against enzyme concentration may be made using simplified data. See Table 4 and Figs. I-7 and I-8. That Emmons obtained a straight line relation between log K_1 and log E is fortuitous and some indication of the insensitivity of a log function of T. Such insensitivity in the measure of enzyme concentration may be responsible for the wide variations in enzyme inactivation reported.

TABLE 4. ILLUSTRATION OF DIFFERENT METHODS OF HANDLING KINETIC DATA FROM CATALASE REACTION

Let A_o = 1.000, A_1 = 0.8, 0.6, 0.4, 0.2 for various concentrations of enzyme (E_1). Then these data may be calculated:

A_1	A_o/A_1	$\log_e(A_o/A_1)$	E(arbitrary units)
0.8	1.250	0.223	1.00
.6	1.667	0.510	2.29
.4	2.500	0.916	4.11
.2	5.000	1.609	7.21

A_1	T	$\frac{100 - T_1}{100 - T_o}$	$\log \frac{(100 - T_1)}{(100 - T_o)} = K_1$	$\log_e E$
0.8	15.8	0.935	-0.0672	.000
.6	25.1	.833	- .1827	.833
.4	39.8	.669	- .4120	1.413
.2	63.0	.410	- .8916	1.975
A_o = 1.0	10.0	--	--	

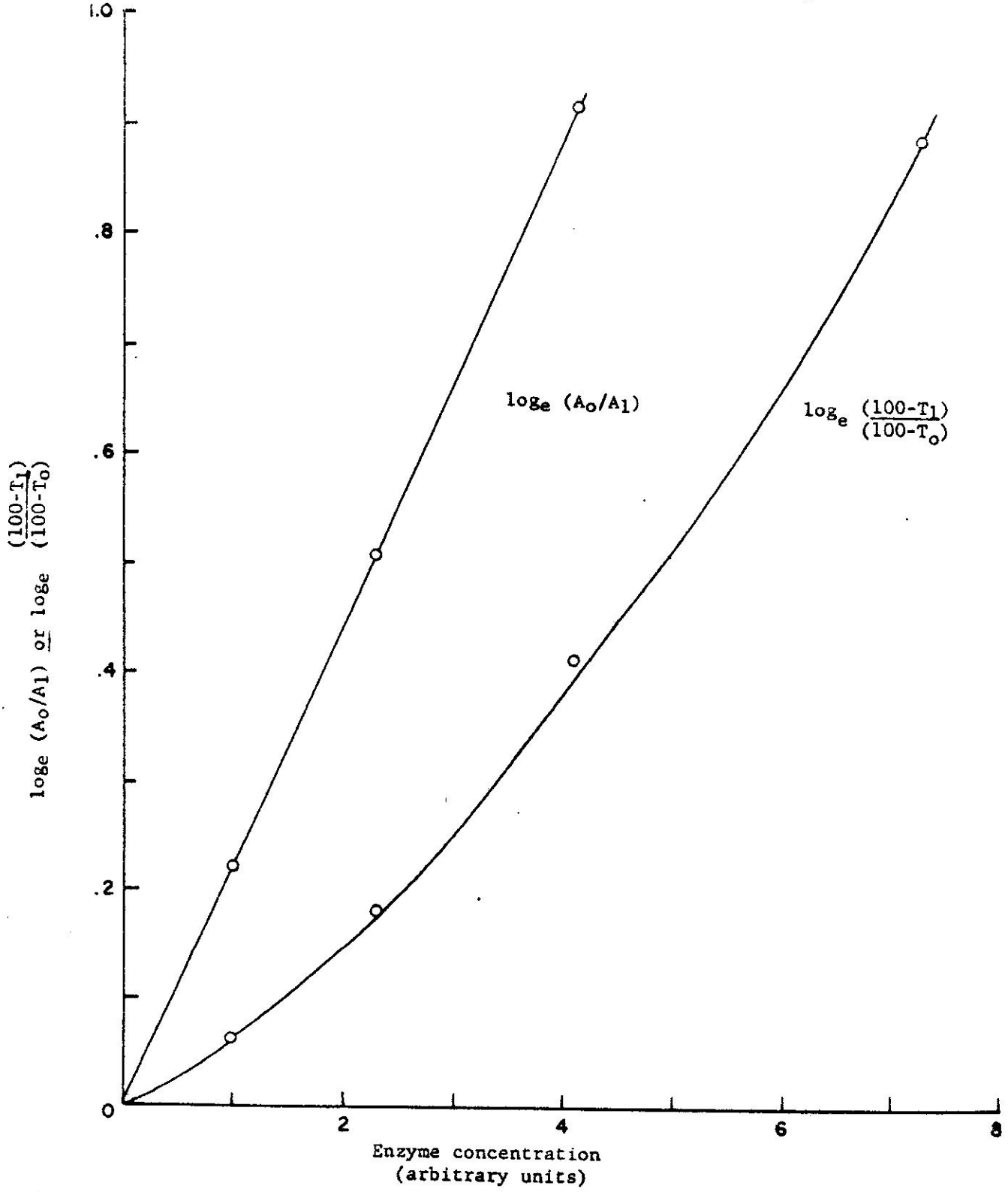

Fig. I-7. Comparison of absorbance and percent transmission plots vs. enzyme concentration

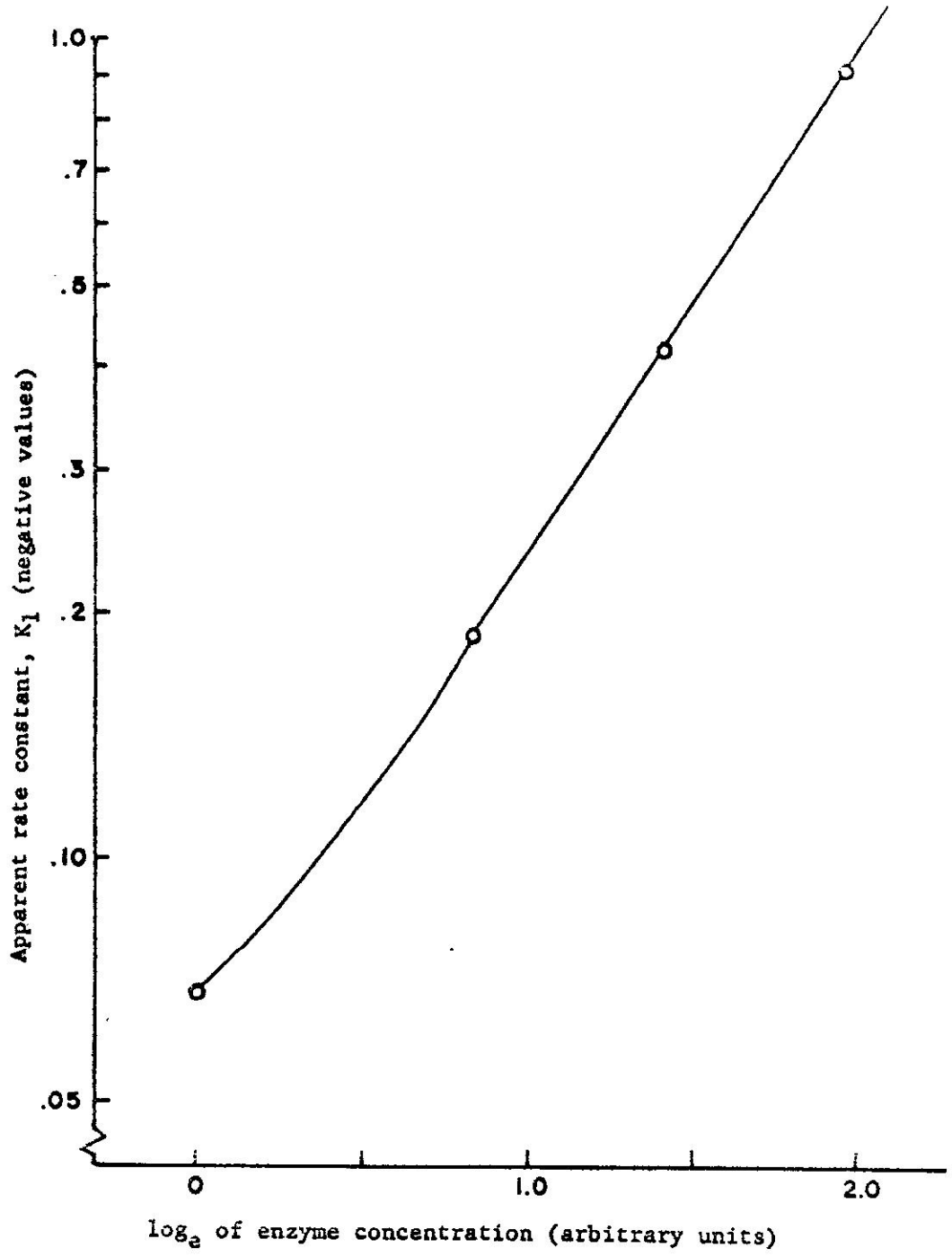

Fig. I-8. Apparent velocity constant vs. enzyme concentration (simplified data)

2. Survey of radiation levels about x-irradiation equipment

A survey of the radiation levels existing about the x-ray spectrometer was made prior to its routine use for irradiations and later after additional shielding was found necessary in the vicinity of the sample holder. A Nuclear-Chicago model 2612 survey meter equipped with thin-window probe for beta-counting was used, and results found are listed in Table 5.

TABLE 5. RADIATION LEVELS ABOUT X-IRRADIATION EQUIPMENT

Location	Counts min^{-1}	Millirad hr^{-1}
Goniometer table, right end, 0-24" above table	100-150	0.3-0.5
Goniometer table, left end, 0-24" above table	100-150	0.3-0.5
Goniometer table, front, 0-24" above table	100-150	0.3-0.5
Goniometer table, in line with second collimator slit, 0-24" above table	5000-20000	2-8
At sample holder, with single shield (3/16" lead sheet) at diffraction crystal	60,000	20
At sample holder, with additional shield at crystal and over second collimator, horizontal	350	1.1
Ditto, vertical measurement	1500	5
Ditto, with additional shielding over crystal and first collimator	1200	4

To minimize the effects of scatter radiation striking the controls and irradiated sample from above, lead shields 1/16" thick were placed atop the compartment in the sample holder.

3. Preliminary experiments on the culture of E. coli[1]

It is desired in the future to test the effect of resonance radiation in in vivo systems. In preparation for this work, the conditions for culture of the unicellular bacterium Escherichia coli were investigated. A culture of E. coli obtained from the U.P.R. Biology Department was inoculated in a sterile medium containing 1000 ml. water, 7.0 g. K_2HPO_4, 3.0 g. KH_2PO_4, 0.5 g sodium citrate $.3H_2O$, 0.1 g. $MgSO_4.7H_2O$, 1.0 g. $(NH_4)_2SO_4$, and 2.0 g. glucose. After 15 days growth at 35°C the culture was stored at 5°C to inhibit further growth. For purposes of counting the cells/ml. of this suspension, a 0.1 ml. aliquot was diluted 1:100, 1:1000, 1:10,000, 1:100,000 and 1:10,000,000. A 0.1 ml. aliquot of each of these dilutions was inoculated with the tip of a pipet on peptone-beef extract agar (Baltimore Bacteriological Laboratories nutrient no. 01-125) in Petri dishes. Samples of 0.1 ml. of sterilized distilled water were used as control. Counting of visually-observable colonies after 2-day incubation at 35°C indicated 1:100,000 dilution would give most accurate plate counts within the standard region of measurement (30-300 colonies per plate). Repetition of this initial experiment using the pour plate modification yielded the data in Table 6. The precision between replicate plates is high, so that this technique should permit a rather sensitive measure of resonant energy effects.

---

1 Carried out by Miss M. Vargas of U.P.R. Chemistry Department.

TABLE 6. PLATE COUNT REPLICATION IN *E. COLI* CULTURING

Sample	Dilution	Colonies/plate
A1	$1:10^5$	175
A2	$1:10^5$	145
A3	$1:10^5$	175
A4	$1:10^5$	168
B1	$1:10^6$	27
B2	$1:10^6$	22
B3	$1:10^6$	22
B4	$1:10^6$	23
C1	control	0
C2	control	1

H. LITERATURE REFERENCES

1) Anon., Spectrometry Nomenclature, Anal. Chemistry 34, 1852 (1962)

2) Beers, R. F., Jr., and I. W. Sizer, "A Spectrophotometric Method for Measuring the Breakdown of Hydrogen Peroxide by Catalase", J. Biol. Chem. 195, 133 (1952)

3) Coombs, T. L., J. P. Felber, and B. L. Vallee, "Metallocarboxypeptidases: Mechanism of Inhibition by Chelating Agents, Mercaptans, and Metal Ions", Biochemistry 1, 899 (1962).

4) Cottin, M. and M. Lefort, "Etalonnage Absolu Du Dosimetre Au Sulfate Ferreux, Rayons X mous de 10 et 8 Kev", J. Chim. Phys. 53, 267 (1956).

5) Emmons, A. H., "Resonance Radiation Effects of Low Energy Monochromatic X-rays on Catalase". Doctoral Thesis - University of Michigan 1959 (also Technical Report #2, Contract No. AT (11-1)-684)

6) Engstrom, L. "Further Studies on the Incorporation of Inorganic Phosphate into Calf-Intestinal Alkaline Phosphatase", Biochim. Biophys. Acta, 54, 179-185 (1961).

7) Hart E. J., et al., "Measurement Systems for High-Level Dosimetry", Proc. 2nd U.N. Intl. Conf. on Peaceful Uses of Atomic Energy, Geneva, 1958. Vol. 21, 188-93.

8) Paraskevoudakis, P., "Resonance in Radiation Effects" Technical Report #5 Contract No. AT (11-1)-684 November 1960.

9) Plocke, D. J., C. Levinthal, and B. L. Vallee, "Alkaline Phosphatase of Escherichia coli: A Zinc Metalloenzyme", Biochemistry 1, 373 (1962).

10) Pribicevic, S. M., O. S. Gal, and I. G. Draganic, "Use of the Fricke Dosimeter for the Measurement of Doses Below 1000 Rads", Report NR-001-0022-1961 Inst. of Nuclear Sciences "Boris Kidrich".

11) Scharf, K., and R. M. Lee, "Investigation of the Spectrophotometric Method of Measuring the Ferric Ion Yield in the Ferrous Sulfate Dosimeter", Radiation Research 16, 115 (1962).

12) Schuler, R. H., and A. O. Allen, "Yield of the Ferrous Sulfate Dosimeter", J. Chem. Phys. 24, 56-9 (1956).

13) Thompson, R. H. S., "Classification and Nomenclature of Enzymes", Science 137, 405-8 (1962)

14) Vallee, B. L., "The 'Active Catalytic Site,' an Approach Through Metalloenzymes", Federation Proceedings 20, 71-80 (1961).

15) Vázquez-Martínez, F., Progress Report No. 1, December, 1962.

16) Westheimer, F. H., in The Enzymes 1, 295 (1959), edited by P. D. Boyer, H. Lardy, and K. Myrback. Academic Press Inc., New York.

CHARACTERIZATION OF A MONOCHROMATIC HIGH INTENSITY VARIABLE WAVELENGTH X-RAY SOURCE IN THE 5-20 KEV REGION

Florencio Vázquez

A. SUMMARY

The x-ray emission system utilized for the present resonance radiation studies has been characterized quantitatively as to intensity and photon energy distribution, and second harmonic contamination.

The monochromatic x-ray beam resulting from crystal diffraction and collimation was analyzed horizontally across its front for a) intensity distribution, utilizing a special moving slit device; and b) photon energy distribution, using double diffraction by a second analyzer crystal.

Estimation of the extent of second harmonic energies was made from a) absorption measurements relying on the different mass absorption coefficients at the first and second harmonic wavelengths and b) double diffraction measurements in which photons with second harmonic energies were analyzed separately. Correction for percentage of reflection by second harmonic energies also was determined by the double diffractometer method. Contamination by higher harmonics was shown to be considerable at higher operating voltages; monochromatic beams can be obtained only by proper selection of tube potential.

The effects on the beam of positioning the various components of the x-ray system (tube, diffraction crystal, two soller slits) were determined and the system was selected which provides high uniformity of photon energy distribution.

As a result, a diffraction system was developed which permits irradiation with photons of uniform energy distribution ($\pm$ 50 e.v. in 6000 - 9000). Such a selectivity of photon energies is not possible with fluorescent emission systems.

B. INTRODUCTION

To study the effect of X-ray irradiation on matter, it is important to know separately the effects of the X-ray energy, the total dose and the dose-rate so as to permit an investigation of the details of the transformations involved and, on that basis, a clear definition of the mechanism for production of change by irradiation.

In particular, we have concentrated on the study of effects produced as a function of X-ray energy. Resonant effects may occur, and it is necessary to utilize an X-ray source in which photon energy can be changed slowly and by appropriate steps.

We must also be concerned with the setting of the irradiating beam at the proper energy and with obtaining the maximum possible intensity. Once these prerequisites are present, we should be able to deliver the required dose in a reasonable time.

Two other important conditions must be met here:

a) Setting the beam as wide as possible in order to avoid the problems arising from very small irradiated samples, and

b) Obtaining a beam of uniform energy and intensity so as to deliver to all particles in the sample, no matter their position, a homogeneous external radiation field.

It is difficult to meet all the above requirements simultaneously because some of them are contradictory. For example, the higher the energy resolution of the beam, the lower the intensity. Also, the continuous range of energies is only possible with lower intensities than those available when discrete emission X-ray energies are utilized. This problem has given rise to two different monochromatic irradiation techniques:

a) The use of high intensities at discrete energy points.

This method was used by M. C. Atkins and W. R. Clendinning.(1)

b) The use of lower intensities, but with almost continuous energy adjustment. This is the technique studied in the present report.

All the work reported was done with a General Electric X-ray diffraction unit XRD-5 shown in Fig. II-1 located in the laboratories of the Department of Physics of the University of Puerto Rico at Mayaguez. Nevertheless our results may be applied to any other similar machine.

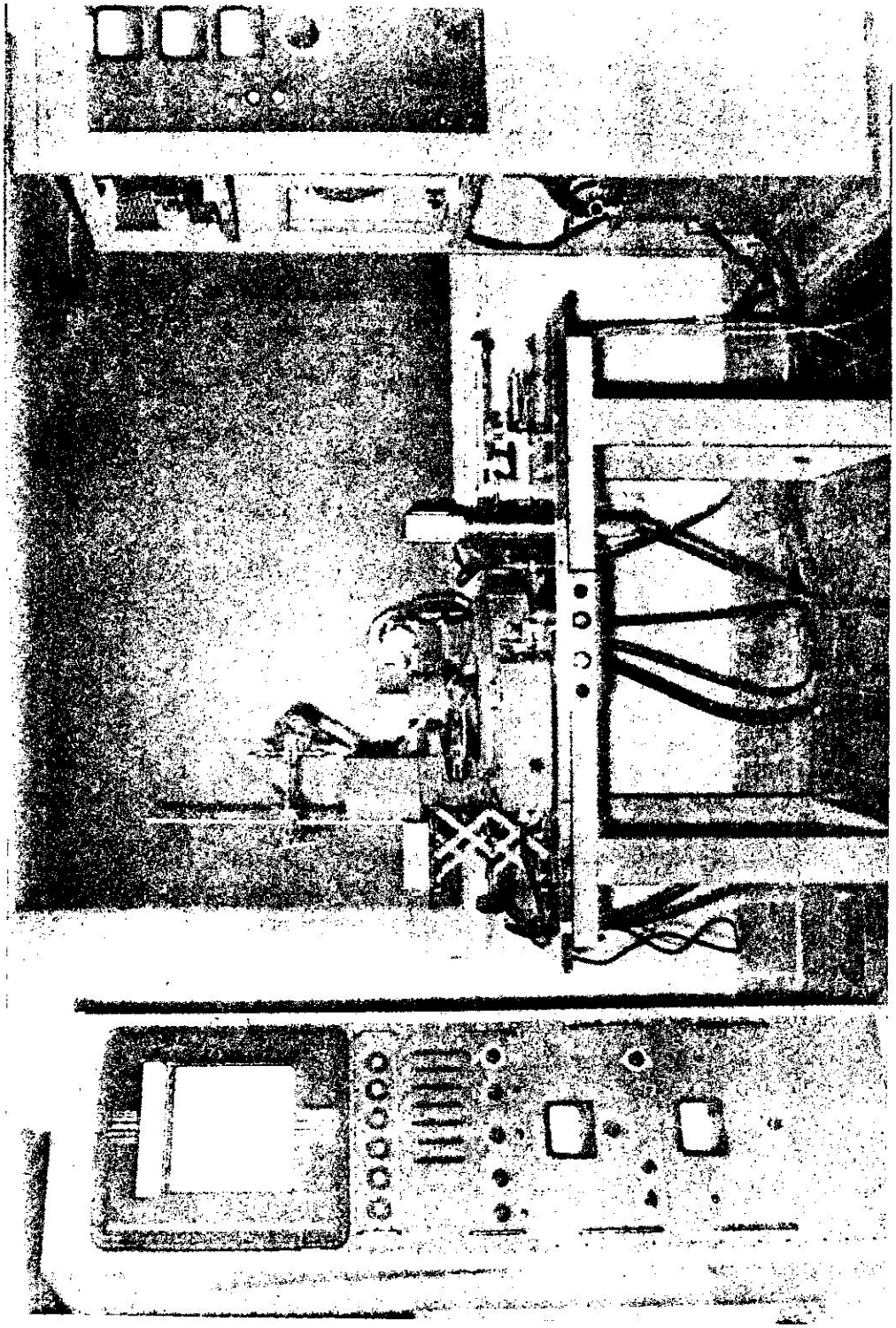

Fig. II-1. Photograph of General Electric X-ray Diffraction Unit XRD-5

C. GENERAL PROPERTIES OF X-RAY PRODUCTION AND DIFFRACTION

Each factor entering into the technique of irradiation, and the relative importance of each factor must be known. Brief descriptions of the most interesting problems involved in X-ray production and diffraction are included here.

1. X-ray production

When, in a X-ray tube, a voltage Vo is applied between the target and the cathode, all electrons coming from the cathode impinge on the target in such a way that photons are produced, with a distribution of intensities and energies.

If we plot the intensities against the energies as shown in Fig. II-2, we get, in general, a continuous distribution of intensity starting at point "A" with peaks at definite energies appearing afterwards.

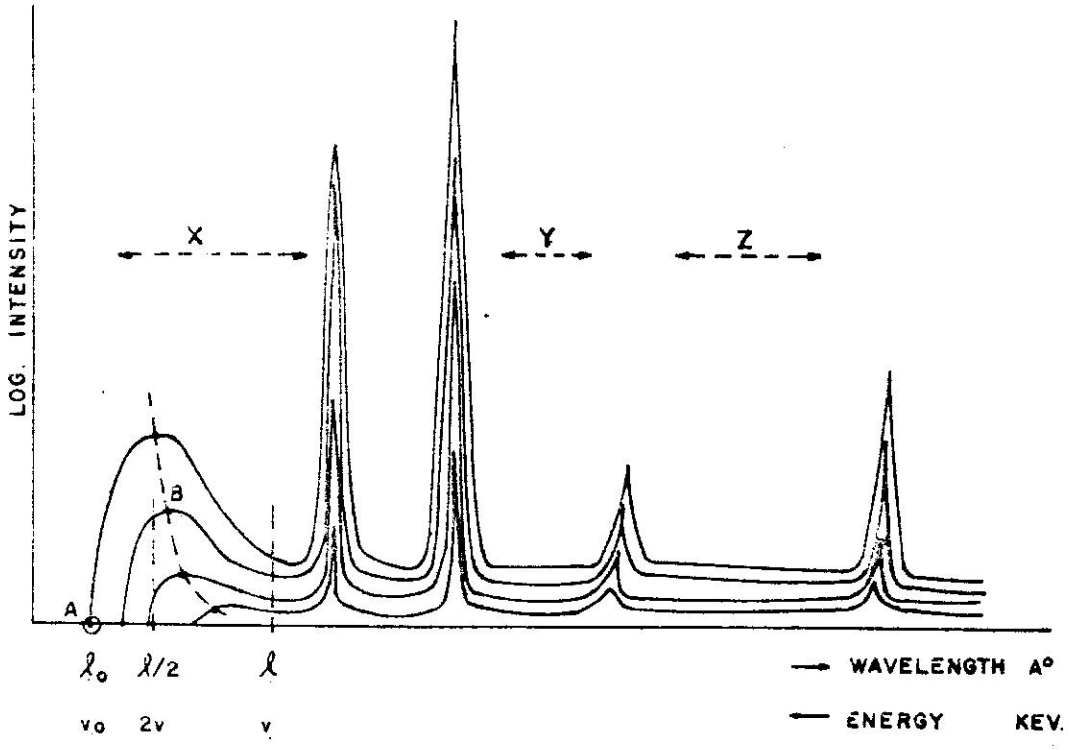

Fig. II-2. X-ray emission distribution

There are two reasons for these two superimposed distributions. When an electron with energy "E" impinges on target it may lose its energy by steps ΔE with the corresponding appearance of photons with energies according to the equation

$$E = h\nu$$

This is the so-called Bremsstrahlung effect. Since the maximum energy of the electron is (V.e) the maximum possible energy of photons is given by:

$$h\nu_o = E = V_o.e$$

and is shown in point A, defined by the applied voltage Vo.

The distribution extends from this limit $h\nu = h\nu_o$ to $h\nu = o$ and is independent of the target material.

There is also the possibility that the impinging electron may eject another electron from any orbit of the target atoms. As soon as the vacancy is produced, an exterior orbital electron falls into it and a photon is produced with an energy given by the difference of the energies of the two corresponding orbits. This last effect is known as the fluorescence effect and is the reason for the high intensity peaks shown in Fig. II-2. For this case, we will get a particular peak if the impinging electron has enough energy to eject the electron of a definite orbit. The peak distribution depends on the electron orbits of target atoms.

Being interested in radiations with a continuous change of energies around a definite value and with constant intensity, we use radiation from the continuous part of the X-ray spectra.

Let us summarize some properties of this part of the spectra.

1.- The intensity in a narrow band of energy $d(h\nu)$ is proportional to the tube power (V.i.)

2.- The total intensity and the intensity in a narrow band are proportional to Z (atomic number of the target)

3.- The limit wavelength of the spectra at point "A" (Fig. II-2) is

$$\lambda_o = \frac{h.c.}{V_o.e} = \frac{12300}{V_o}$$

where λ_o is given in Angstrom units when V is expressed in volts.

4.- For a particular energy ($h\nu$), according to the voltage applied, the tube can emit harmonics of the first energy, given by $2h\nu$, $3h\nu$, and so on.

5.- As the maximum voltage applied to the tube is increased, the spectra shift to the left as can be seen in Fig. II-2. The peaks in this figure do not correspond to any specific atom but are "representative". It can be seen that the useful zones of irradiation are those labelled x, y, z. For these the intensity distributions are almost uniform, with maximum intensities near the spectrum limit, as should be the case.

2. X-ray diffraction

An X-ray beam incident on a crystal is diffracted according to Bragg's Law:

$$n.\lambda = 2d \sin \theta$$

where n is an integer, λ is the wavelength of diffracted X-rays, d is the interplanar spacing between successive atomic planes in the crystal and θ is the angle between the atomic plane and both the incident and the reflected beams.

The beam obtained after diffraction is monochromatic with the following limitations:

1.- As the incident angle is defined by slits with a definite width the diffracted beam also has a band of photon energies $h\nu \pm \Delta h\nu$ according to the incident angles $\theta \pm \Delta\theta$.

2.- The crystal produces dispersion which also causes energy diffraction.

3.- If there are photons in the incident beam with energies $2h\nu$, $3h\nu$ --- $nh\nu$, they are also diffracted.

4.- In diffraction the intensity of the incident beam is strongly reduced. The percentage diffracted is quite dependent on the type of crystal. Also, depending to the crystal, the percentage diffracted is quite different for fundamental, second, third --- harmonics, in such a way that some crystals strongly reduce diffracted harmonics.

5.- The Bragg equation limits to 2d the maximum wavelength that can be measured with a given crystal, since sin θ cannot exceed unity.

6.- A relation between the width of the beam and the length of the crystal is easily observed in Fig. II-3.

7.- The analyzer crystal, by its atomic structure, determines the

the efficiency of the crystal is not very high, but it can vary substantially from one crystal type t another. Selection of the crystal is therefore an important decision.

Two theories have been developed to explain analyzer crystal reflecting power. The first, developed by Darwin and quoted in James (8) assumes that the crystal consists of perfect parallel planes of atoms with equal spacing between planes:

$$R_p = \frac{8}{3\pi} \frac{e^2}{mc^2} N \lambda^2 |F| \frac{1 + |\cos \theta|}{2 \sin 2\theta}$$

where R_p is the reflecting power of the "perfect" crystal

λ is the wavelength diffracted

N is the number of atoms per unit volume

$|F|$ is the atomic scattering factor for the diffracted wave direction 2θ. $|F|$ has a maximum value of Z for angle $2\theta = 0$, and decreases as 2θ increases.

$\frac{e^2}{mc^2}$ is the classical "electron radius"

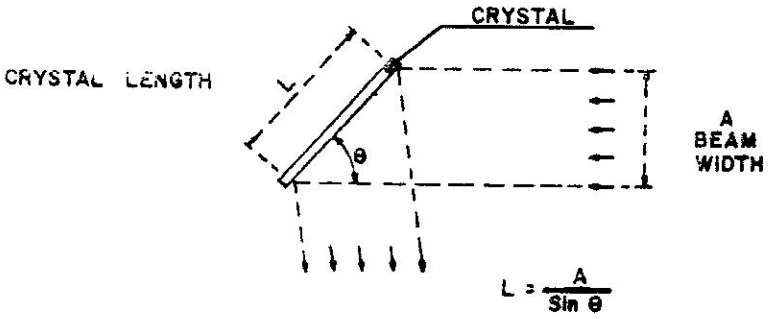

Fig. II-3. Crystal Length

structure in the crystal; the crystal consists of small "crystallites", each slightly skewed from the average direction for the group as a whole:

$$R_m = \frac{e^2}{mc^2}^2 \frac{N^2 \lambda^3}{2\mu} |F|^2 \frac{1 + \cos^2 2\theta}{2 \sin 2\theta}$$

where R_m is the reflecting power of the "mosaic" crystal

μ is the linear absorption coefficient of the crystal for x rays of wavelength

N is the number of unit structural groups (crystallites) per unit volume

F is the scattering factor for the structural group and may be written $\sum_i f_i \ e^{-M_i}$.

Here f_i is the scattering factor of the "i" atom, and approaches Z for small angles provided λ is much shorter than the absorption wavelengths of the atom. The term e^{-M_i} corrects for the temperature of the crystal. For our work, this factor may be neglected.

Note that R_p contains the number of atoms (or electrons) per unit volume and the scattering factor f , which is also proportional to Z. However, Rm contains both factors to the 2nd. power. Thus, Rm will always be much larger than R_p. In nature, most crystals are much closer to "mosaic" in structure.

Adopting Rm, calculations were made for crystals of Lithium Fluoride, Aluminum, Sodium Chloride and Quartz. The corresponding values of Rm are:

Li F (200) - 1543×10^{-6}

Al (111) - 670×10^{-6}

NaCl (200) - 560×10^{-6}

Quartz (1011) 490×10^{-6} (experimental)

These indicate that, for a wavelength of 1.739 A° (K absorption edge of iron), a Lithium Fluoride crystal is superior. In this case, μ, the linear absorption coefficient is small, and the number of atoms per unit volume is high. This is sufficient to compensate of the smaller number of electrons per atom. However, the diffracted energy is still only a small part of the incident energy.

D. INTENSITY AND ENERGY DISTRIBUTION

Most of the studies in this section were made with two special devices built in our shops. The first provides for detailed measurement of intensity distribution across the diffracted X-ray beam.

The second device is used to analyze the photon energy content at all points across the beam. Both instruments are described below.

1. Intensity distribution

A photograph of the device used is shown in Fig. II-4 with the corresponding sketch in Fig. II-5.

The device replaces the normal support of the X-ray detector geiger counter with a two section mechanism. The lower section is fixed to the goniometer protractor and the upper section carries the geiger counter in such a way as to provide a sliding motion normal to the X-ray beam. A lead screw moves the counter to the desired position. The window of the counter is covered with a shield containing a well-defined slit. Photons from the beam enter the counter only through this slit. By sliding the window slit across the beam, and counting at different points, the intensity distribution can be established.

If the width of the window slit is much less than the width of the individual medium resolution (MR) soller slits we can also get the intensity distribution across the individual soller slits, as shown in Fig. II-6, A_1. Here, each maximum corresponds to the center of a soller slit. If the width of the window slit is similar to that of the MR soller slits, we obtain a mean intensity distribution across the beam like that drawn in Fig. II-6, B_1. Fig. II-6, C_1, shows, at the bottom, a crossection of the soller slit assembly and, at the top, a film negative taken at the

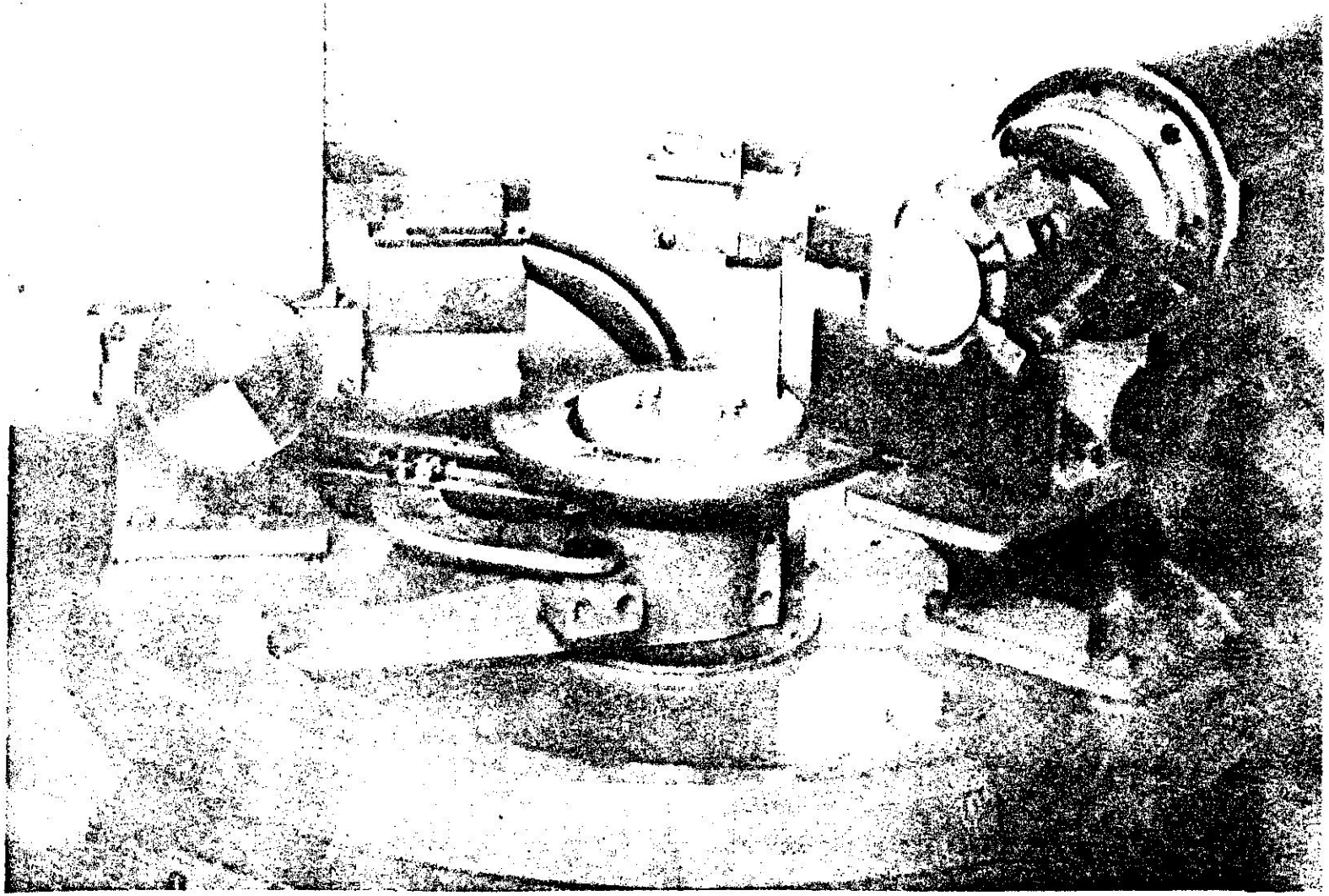

Fig. II-4. Photograph of the diffraction unit with counter on sliding device

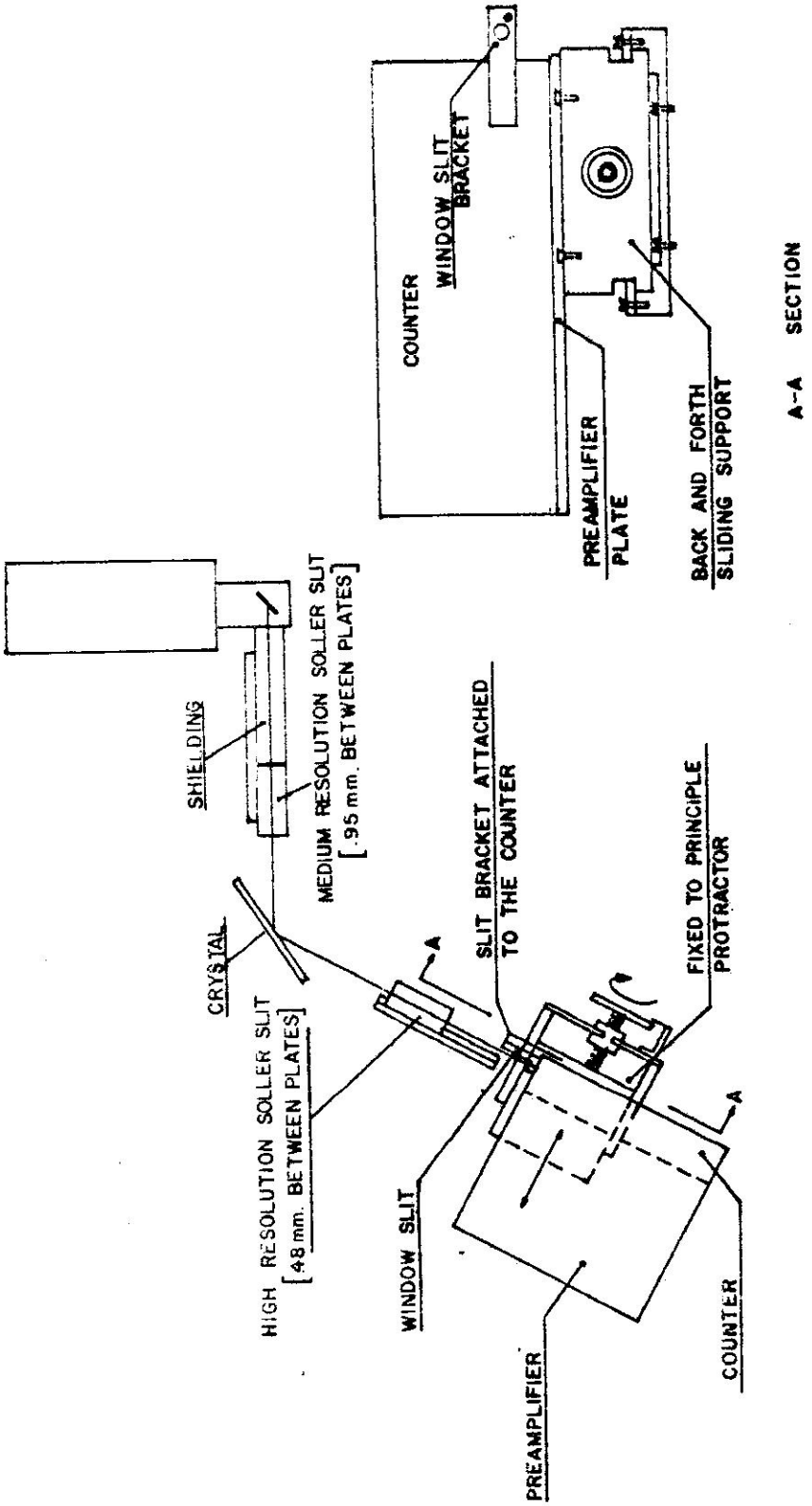

Fig. II-5. Sliding device sketch

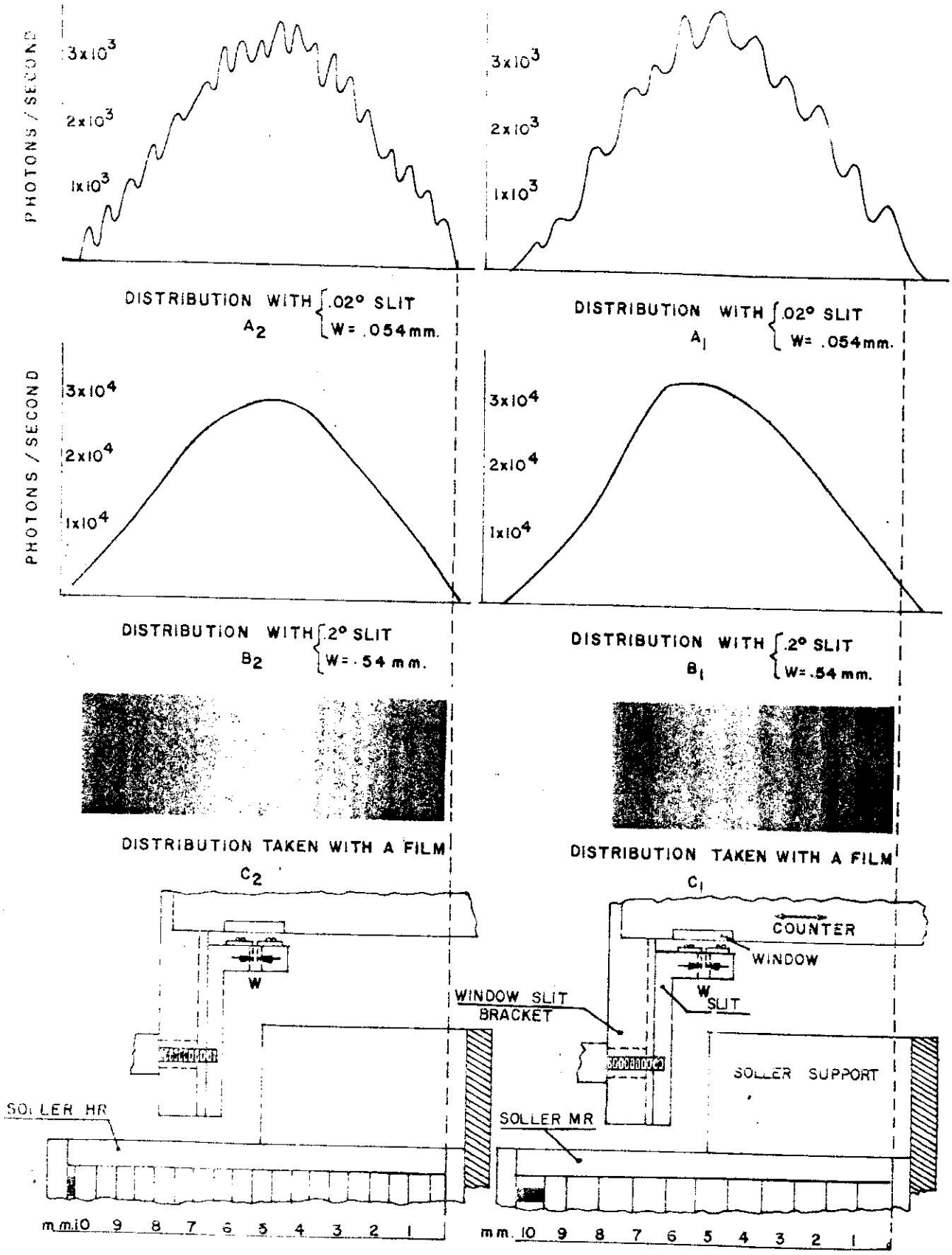

Fig. II-6. Intensity distribution

sample position. It can be seen how the shadows in the film coincide with the MR soller slits.

Fig. II-6, A_2, B_2 and C_2, show similar diagrams for the case of the high resolution soller slit system. Here, 19 maxima occur, corresponding to 19 soller slits. The MR soller contains only 9 corresponding slits.

The intensity of the whole beam can be obtained by integrating under the curves. If the slit has a width $\underline{w}$, the distance between two consecutive counting points is $\underline{b}$, and the measured intensities are given by S_1, S_2, --- S_n, then the total intensity is:

$$S = S_1 \frac{b}{w} + S_2 \frac{b}{w} + \text{---} + S_n \frac{b}{w} = \frac{b}{w} \sum_{i=1}^{i=n} S_i$$

It should be noted that we obtained the same results, within a 0.3% difference with the narrower slits as with the wider slits, when corrections for the dead time of the counter were made. Using reading periods of 10 seconds duration, the intensity of the whole beam was obtained with good statistical accuracy.

A similar procedure was used in comparing intensities for the different cases.

2. Double diffraction - Photon energy analysis.

In order to determine energy distribution of the beam, a special crystal analyzer device was used. It is shown in Fig. II-7 by a photograph, and in Fig. II-8 by a sketch.

The device consists of a steel plate "A" which can slide in direction a-a (normal) across the beam. A rotating crystal holder, which is an accessory normally used in spectrometer techniques, is mounted on top of the plate. After fixing the base, the crystal is moved into

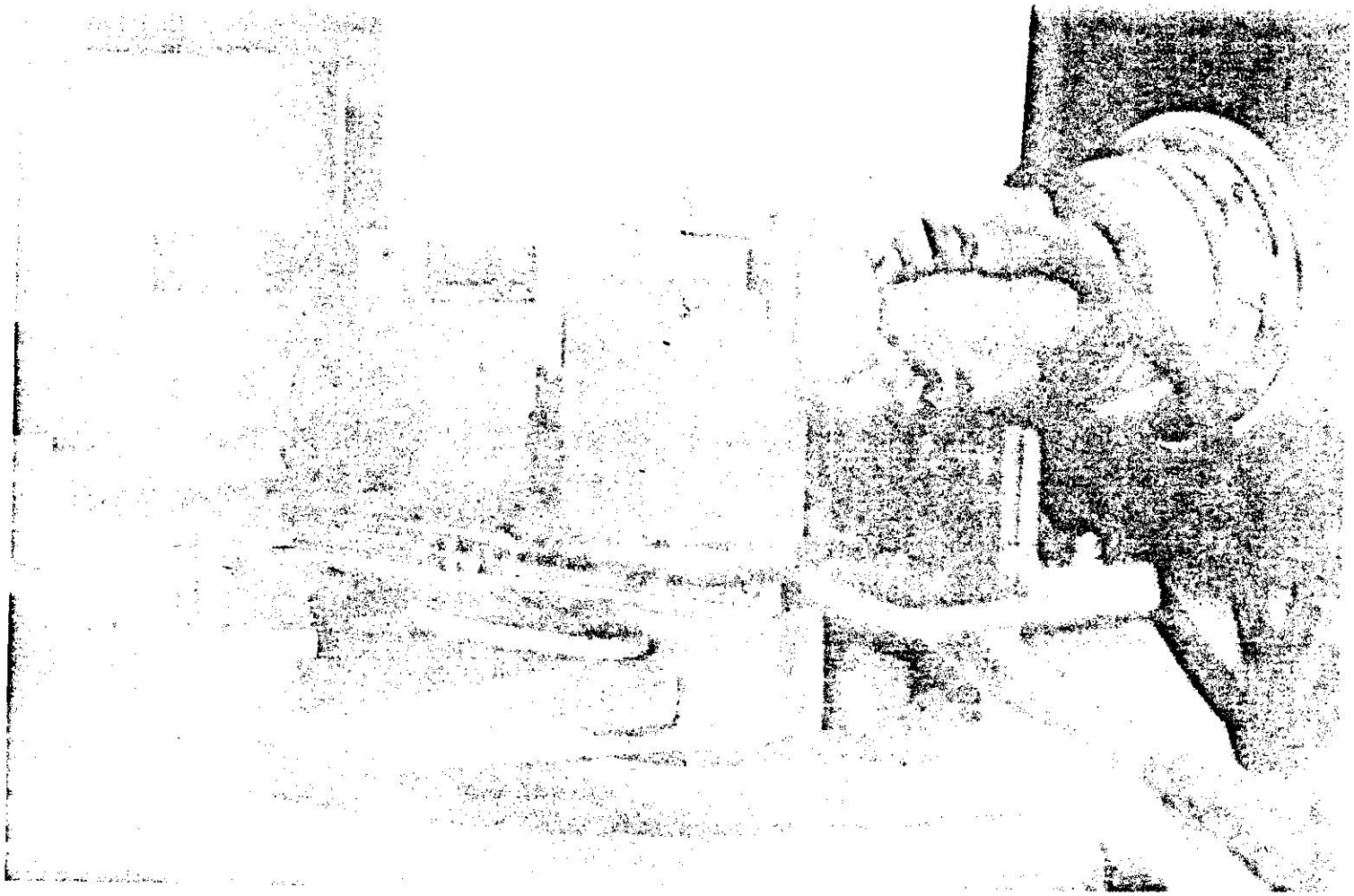

Fig. 11-7. Photograph of diffraction unit with double diffraction device

exact axial position in the beam by means of a lead screw, providing motion in direction "a-a". Precise setting of the corresponding angle desired is obtained from the rotary table of the crystal holder. A support bracket holds a shield and slit in such a way that photons which arrive at the second crystal have come from the first crystal without intervening scatter.

A counter is mounted on the plate, in such a way as to permit rotation around the crystal axis. It is turned by means of a circular steel strip and a screw, as shown in Fig. II-8. Another slit and shield are attached to the counter so as to block scattered radiation from the first crystal.

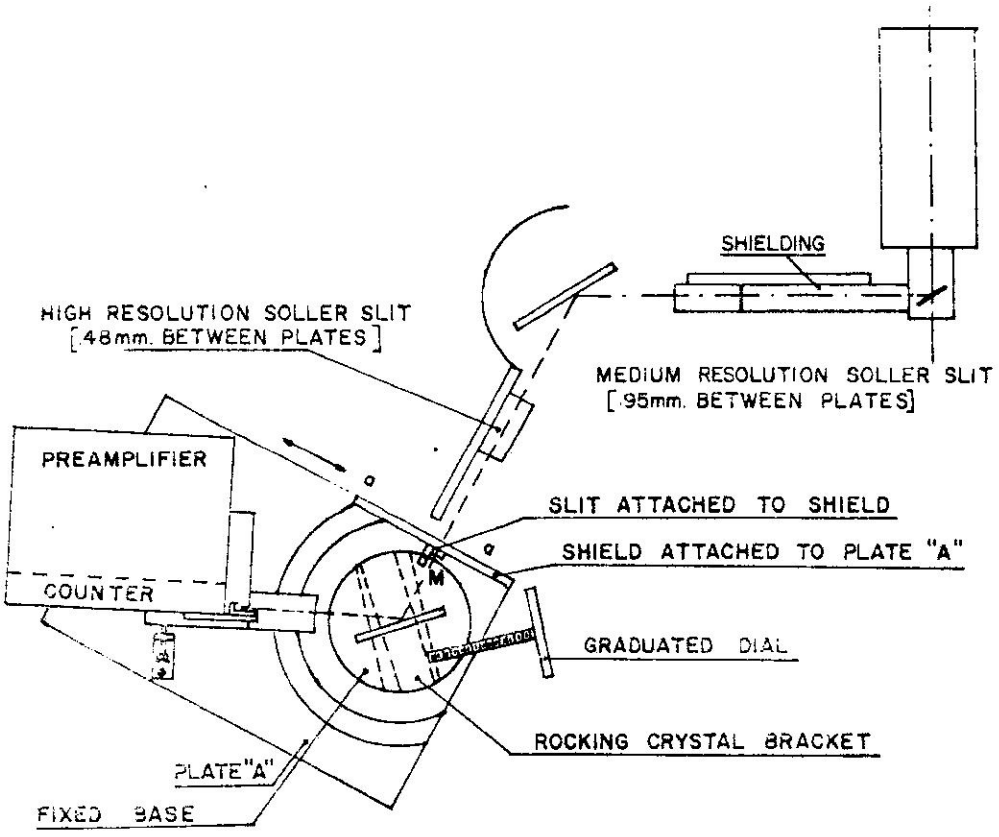

Fig. II-8. Double diffraction device

2. CHARACTERISTICS OF X-RAY TUBE

Much of the research in this study has been done by irradiating at energies close to the K absorption edge of a particular atomic element. Once the X-ray energy around which we are to irradiate is decided, the next problem is selection of the appropriate X-ray tube anode. Some of the criteria for the selection are commented on briefly below.

1. Selection of anode material

The higher the atomic number of the anode the higher the radiation intensity, at any fixed values of anode voltage and current. However, since we wish to adjust the energy of the radiation reaching the material under study, the output should change slowly as a function of energy. The anode material should be free of strong sharp emission lines in the energy region under study. (See Fig. II-2)

2. Operating voltage

A precise determination of the anode voltage to be used can be made only after the permissible second harmonic contamination has been established. As a starting point, we can apply a voltage giving twice the minimum photon energy desired, since up to this value, no second harmonic is generated for the energies under study. This problem is discussed in detail in a later section.

3. Operating current

Once the voltage and the anode material have been selected, the maximum operating current is determined on the basis of either the maximum allowable anode-power dissipation or the maximum filament current permitted. These vary with the tube type. Our present equipment allows up to 50 ma. anode current. We plan to install new 100 ma equipment soon.

4. Output pattern and collimation

The next step is the measurement of the output pattern, which in turn determines the arrangement of collimators in the diffraction unit. In the usual diffraction study, small areas and narrow slit openings are used to obtain high spatial resolution. In emission studies, narrow slit systems are used to resolve emission lines. However, our objective is maximum flux commensurate with good energy resolution. We have used medium resolution soller slits before the crystal and a high resolution set after the crystal. The slits are set in the vertical position. This arrangement yields the maximum useful output. The monochromaticity of the output was checked using double diffraction as described above.

5. Anode shape and orientation

The importance of the atomic number of the anode material was mentioned earlier. We will now consider the form of the anode surface. The General Electric CA-7 tube has a target which is 0.8 x 15 mm. and windows which are disposed as shown in Fig. II-9. The surface of the target is perpendicular to the longitudinal axis of the tube. Fig. II-9 also shows the emission pattern; taken with two films at the normal position of the first soller slit. We found that with window B the soller was not well filled, but with windows A and C, the results were much improved.

The General Electric AEC 50-T tube has a target which is 5 x 5 mm. in projection and forms an angle of 70° with the tube axis. This angle is important from the viewpoint of getting higher intensities, a question which will be considered in the next section. The effect of a large projected area across the width of the soller slit is to promote uniform intensity.

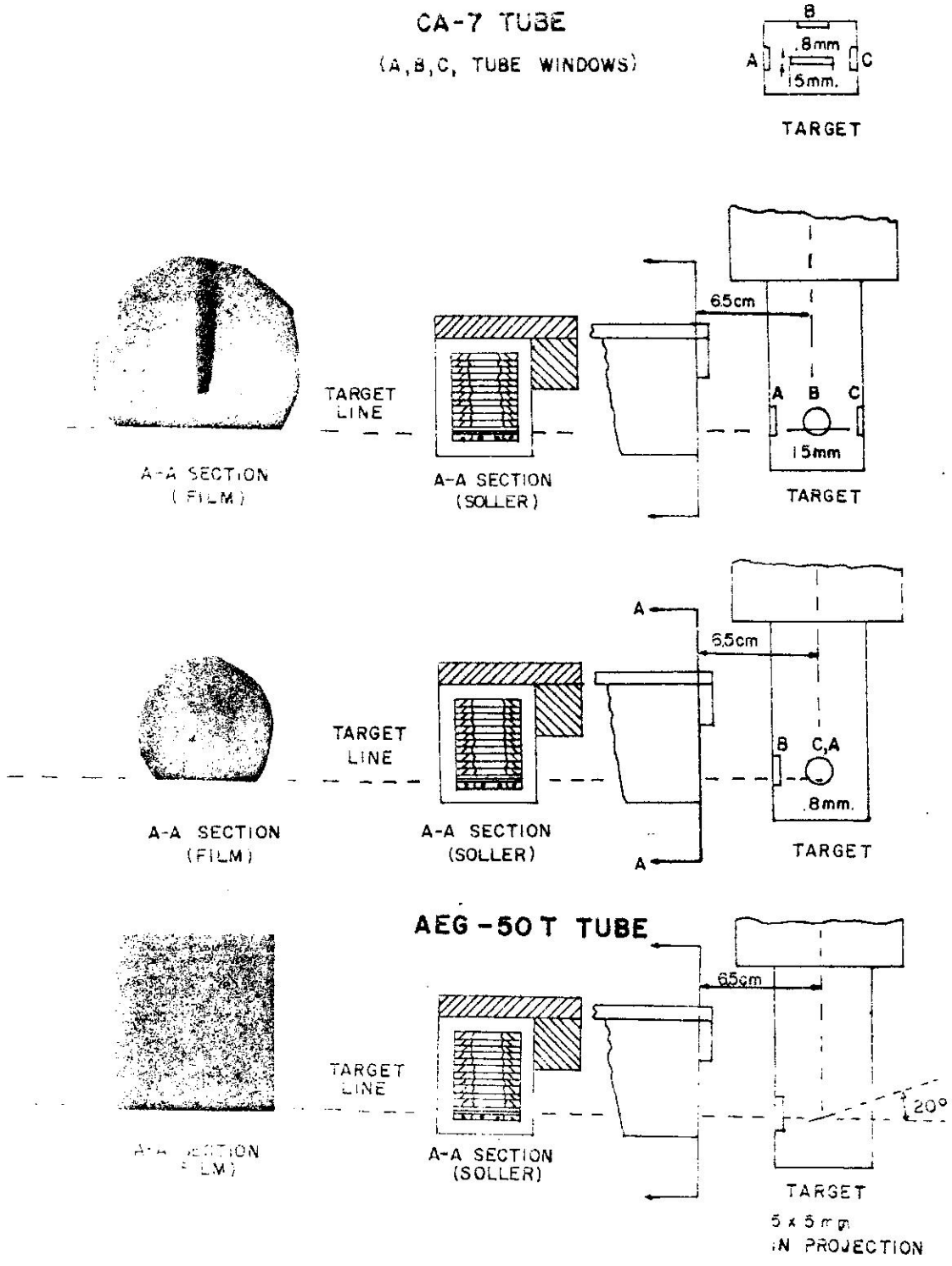

Fig. II-9. Target emission patterns

F. ANALYSIS FOR HARMONICS IN X-RAY BEAM

As was stated earlier, the higher the voltage applied to the tube, the higher the intensity obtained. However, there exists a potential V_o above which the beam contains higher harmonics, which are not wanted. We must, therefore, determine the maximum voltage that can be applied, taking into account the percentage of second harmonic which can be tolerated.

Two methods were used to find the percentage of second harmonic present. The first one is based on the different mass absorption coefficients of an absorber for two different wavelengths. The second is based on double diffraction.

1. Absorption method

Let us suppose that the diffraction unit is arranged for irradiation as shown in Fig. II-10.

The problem is to find at a point A, where the sample is to be placed, the percentage of the second harmonic as a function of voltage. Since the position of the counter is close to point A, the intensity of the beam is the same as that received by the counter.

Hence if I_1 is the intensity as measured by the counter, then;

$$(1) \quad I_1 = I_\nu \alpha + I_{2\nu} \beta$$

where α and β are the efficiencies of the counter for energies ν and 2ν obtained from manufacturer.

If we put in place "B", an absorber with a large difference in the absorption coefficient for the energies ν and 2ν, and in which energy ν is more strongly absorbed, then the intensity as given by the counter will be

$$(2) \quad I_2 = I_\nu \alpha \, \bar{e}^{\left(\frac{\mu}{\rho}\right)_\nu \rho d} + I_{2\nu} \, \bar{e}^{\left(\frac{\mu}{\rho}\right)_{2\nu} \rho d}$$

in which:

a) $(\frac{\mu}{\rho})_{\nu}$ and $(\frac{\mu}{\rho})_{2\nu}$ are the mass absorption coefficients for energies ν and 2ν

b) ρ is absorber density

c) d is absorber thickness

From equations (1) and (2) we get

$$\frac{I_{2\nu}}{I_{\nu}} = \frac{\alpha}{\beta} \frac{e^{-(\frac{\mu}{\rho})_{\nu} \rho d} / I_2/I_1 - 1}{1 - \frac{e^{-(\frac{\mu}{\rho}) 2\nu \rho d}}{I_2/I_1}} = \frac{\alpha}{\beta} \frac{\frac{A}{I_2/I_1} - 1}{1 - \frac{B}{I_2/I_1}}$$

With d fixed, values of the factors A and B may be calculated with the aid of tables of monochromatic absorption coefficients or by measurement, using the X-ray unit.

If direct measurements are made for a given frequency, ν, the X-ray unit must be operated initially at a voltage lower than V_o, at which the second harmonic will appear.

The intensities I and I_o, with and without the absorber, are measured to obtain,

$$I / I_o = \bar{e} \, (\frac{\mu}{\rho})_{\nu} \, \rho d \cdot$$

To obtain the second factor, the spectrometer angle is set for frequency 2ν and a voltage above V_o but less than $2V_o$ is used.

Once we have the two factors needed and the α, β efficiencies of the counter, determinations are made of I_2/I_1 at different voltages so as to obtain the percentage of second harmonic present.

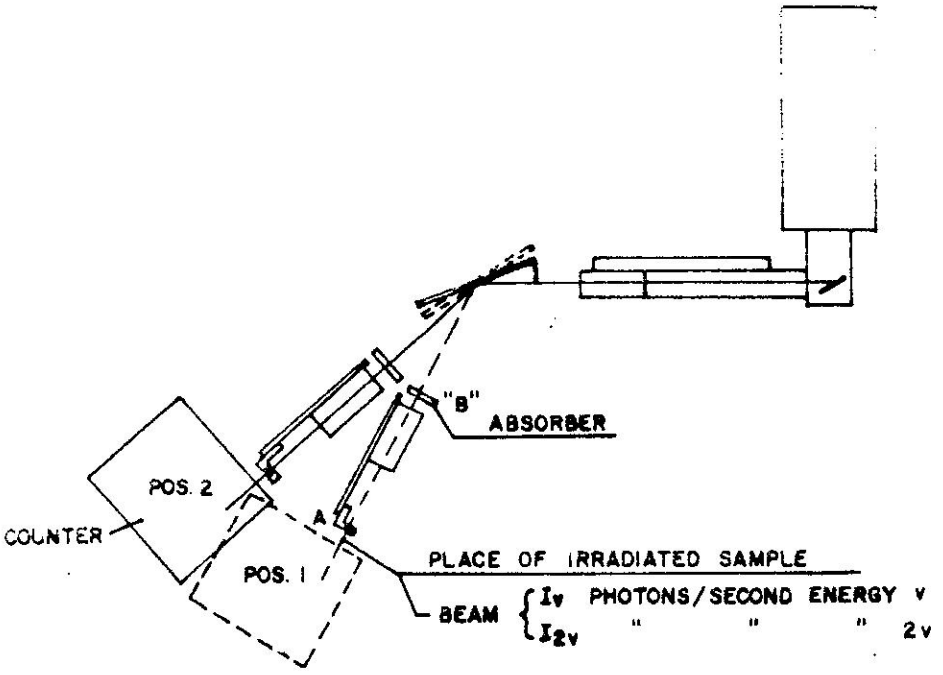

Fig. II-10. Component orientation for second harmonic studies (absorption method)

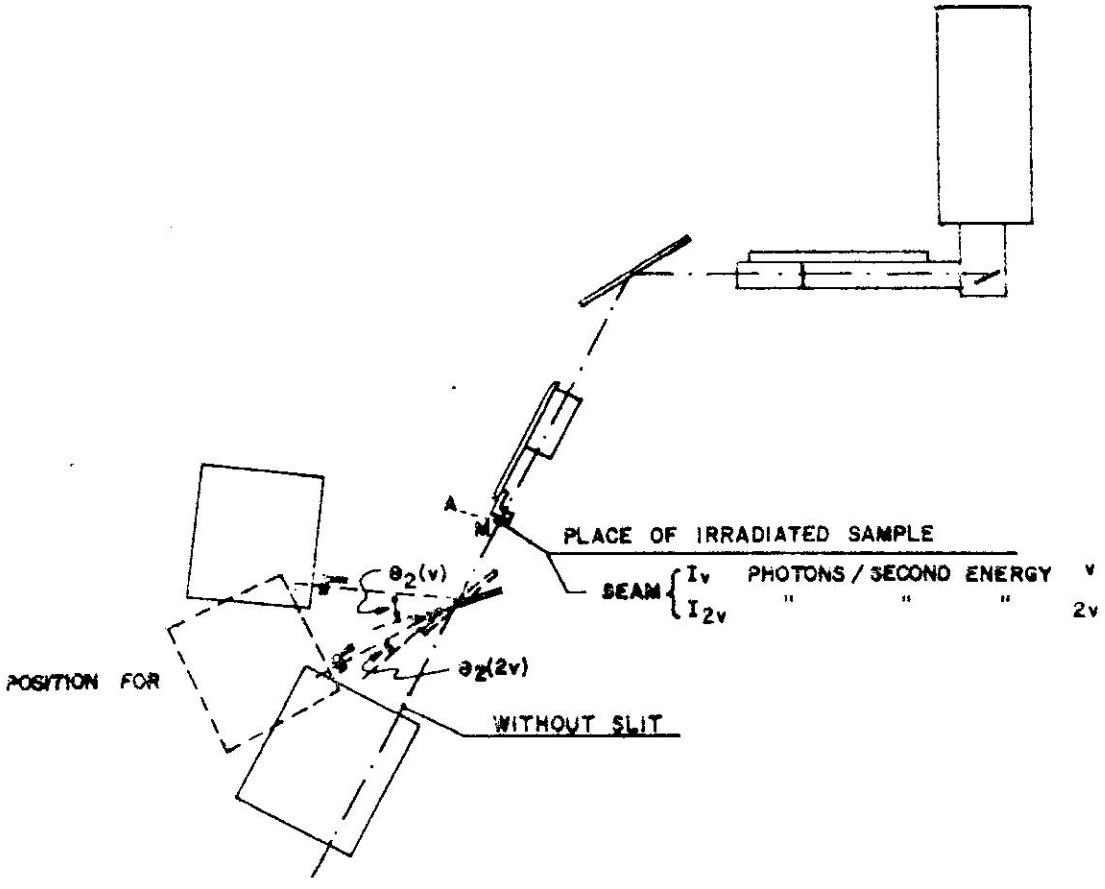

Fig. II-11. Component orientation for second harmonic studies (double diffraction method)

2. Double diffraction

For this method, the proper arrangement of the main diffraction unit and the added double diffraction unit are as shown in Fig. II-11.

Let us suppose line A-A to correspond to the front surface of the sample, and let us select with a slit in point M a fraction of the total beam which we are to analyze. Also, let us suppose the mixed beam to be composed of intensities I_ν and $I_{2\nu}$. Placing a second crystal with appropriate angle $\theta_2(\nu)$ to diffract energy ν, and measuring $I_1(\nu)$ intensity at the counter, we have

$$(1) \quad I(\nu) = \frac{I_1(\nu)}{\eta_{cr}(\nu)\eta_{co}(\nu)}$$

where

$\eta_{cr}(\nu)$ is the crystal percentage of reflection and

$\eta_{co}(\nu)$ is the counter efficiency

In the same way, with the crystal in position $\theta_2(2\nu)$ we get

$$(2) \quad I(2\nu) = \frac{I_1(2\nu)}{\eta_{cr}(2\nu)\ \eta_{co}(2\nu)}$$

Hence the percentage of the second harmonic present is given by

$$(3) \quad \frac{I(2\nu)}{I(\nu)} = \frac{I_1(2\nu)\eta_{cr}(\nu)\eta_{co}(\nu)}{I_1(\nu)\ \eta_{cr}(2\nu)\eta_{co}(2\nu)}$$

For precision measurements, it is necessary to take into account different absorption by air of photons with energies ν and 2ν between point A and counter. However, by computation the above was found to be unnecessary, because of the short distance between the crystal and the counter.

Another important correction must be made for the second harmonic photons measured in $I_1(\nu)$. The correct equation should be

$$(4) \quad I(\nu) = I_1(\nu)\ \eta_{cr}(\nu)\eta_{co}(\nu) + I_{2\nu}\eta'_{cr}(2\nu)\eta'_{co}(2\nu)$$

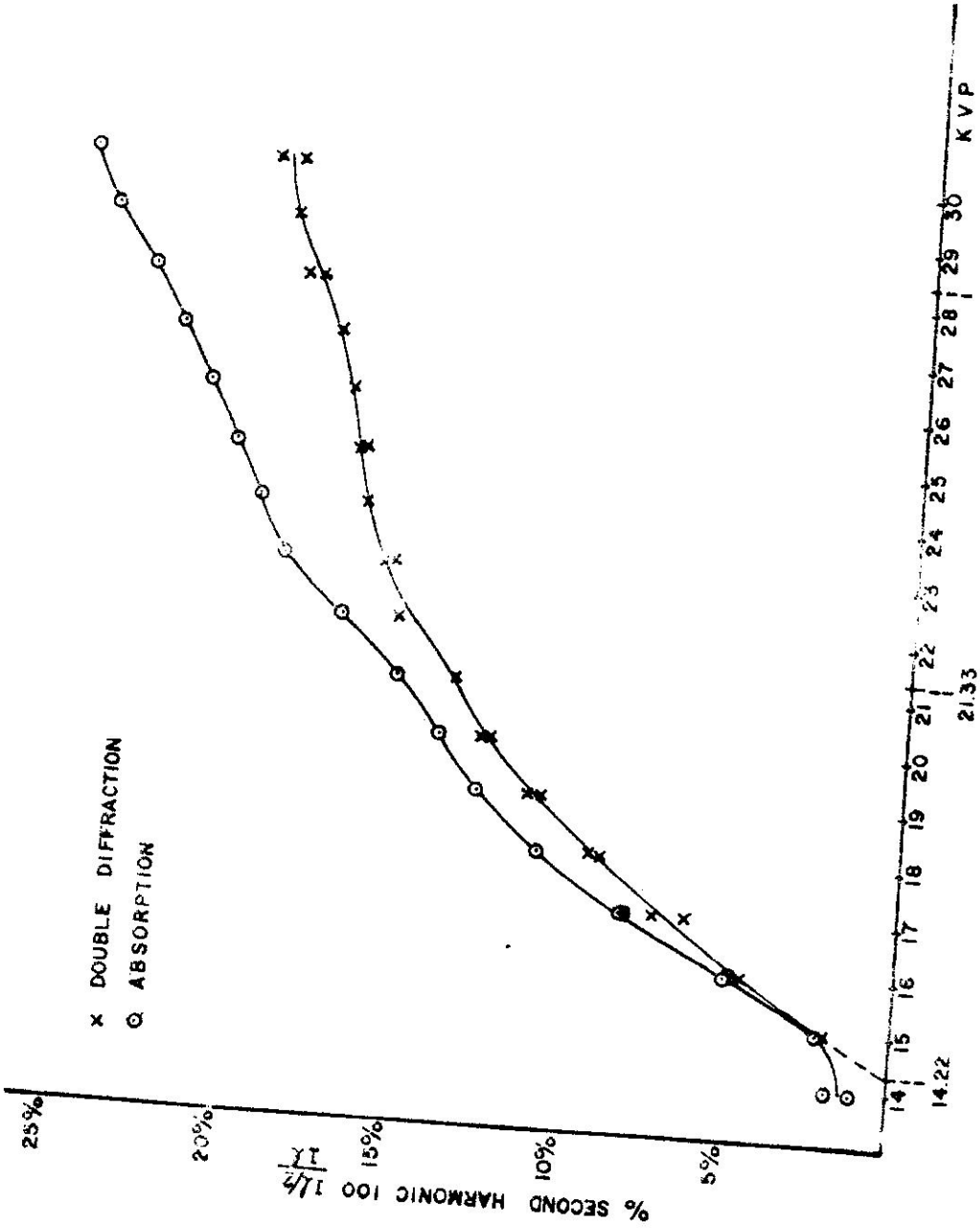

Fig. II-12. Percentage of the second harmonic contamination

is more accurate in that it accounts for the value of 14.22 KVP, which is the starting point for second harmonic production. The curves were taken with the crystal set to diffract 7.111 Kev energy photons. Both curves change slope at about 21 KVP and 28.5 KVP, which indicates the appearance of the third and fourth harmonics at these operating voltages.

Both curves are similar at the lower voltages, hence both methods cross-check each other. For the higher voltages it is necessary to use Eqtn. 4 instead of Eqtn. 1.

In the present problem where we were interested in avoiding all second harmonics, the voltage 14 KVP was chosen for all irradiations.

G. ORIENTATION OF X-RAY TUBE, PROTRACTOR, AND SOLLER SLITS FOR OPTIMUM INTENSITY AND RESOLUTION

In the following sections the relative positions of the spectrometer elements are studied with the general objective of getting the highest possible uniform distribution of intensity. Particular attention is given to obtaining maximum energy resolution.

Analysis of the general procedure is best made by following the steps used in the particular case of irradiating at the K absorption edge of iron.

1. Tube position

The X-ray tube must be positioned correctly to obtain a symmetrical intensity distribution.

To obtain a symmetrical distribution along the height of the soller slit, it is necessary to place the tube with target surface parallel to the rotation axis of the crystal. The centerline of the soller must be at the same level as the center of the target. This adjustment is made with screws M, N, P, Q and with the levelling screws A, B, C, as shown in Fig. II-13.

The tube position may be changed, in addition, by rotating it a few degrees around an axis perpendicular to the plane of the figure. This last possibility is limited by the tube holder walls and by the insulation of the high tension cable. The advantage gained in putting the tube in such a skewed position is a slightly larger angle between the target surface and beam center line, thus increasing the flux into the soller collimator. When the target plane of the tube is perpendicular to the tube axis, this device may be useful. There are other techniques and adjustments for this type of tube, described in later sections, which also may be used to increase useful output.

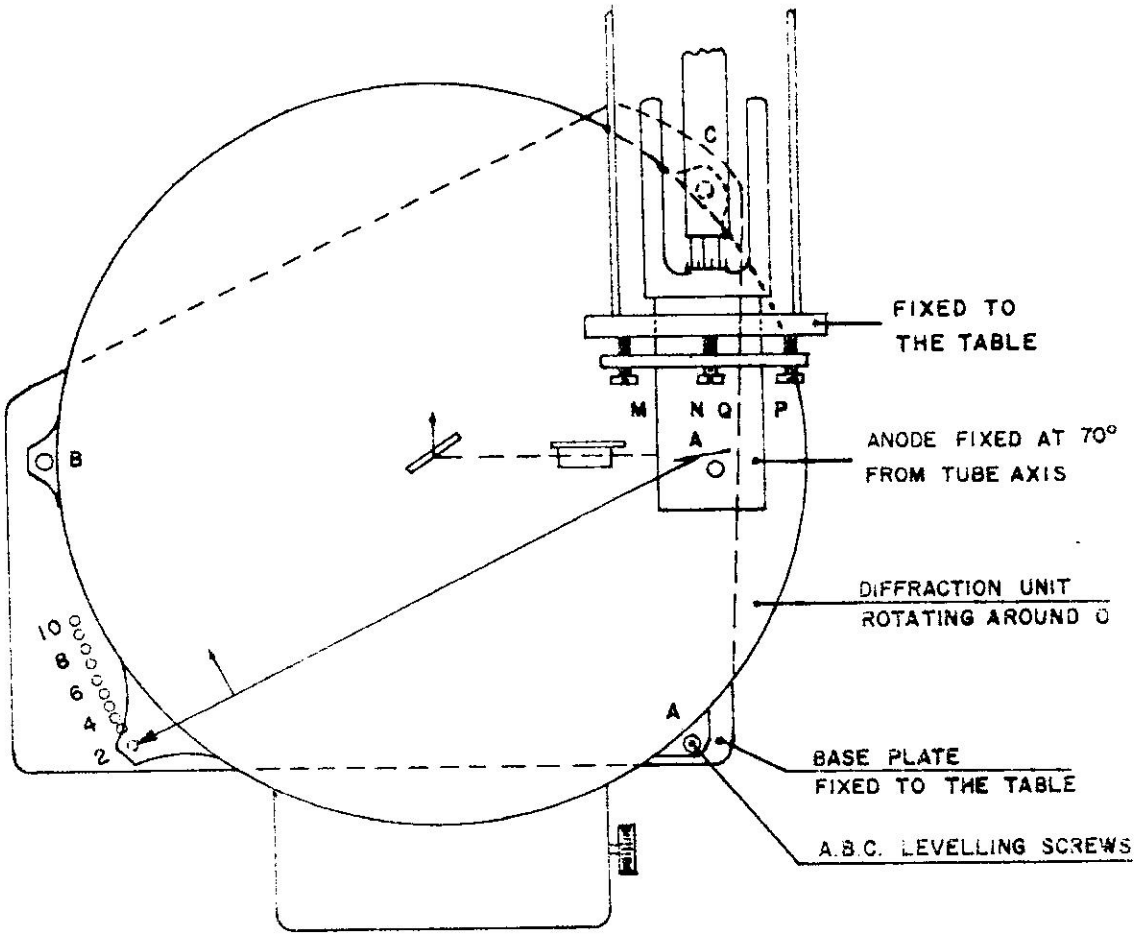

Fig. II-13. Tube and diffraction unit with small protractor

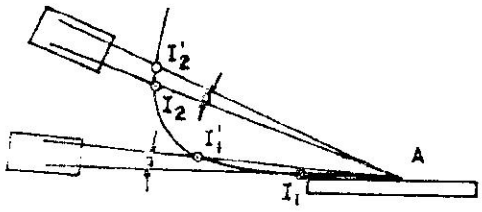

Fig. II-14. Target angular intensity distribution

In the case of a tube with the target plane at an angle of about 20°, the additional angle obtained in the skew position is insignificant.

The G. E. X-ray tube CA-7 has a flat anode. This tube is ordinarily used for crystal structure diffraction studies. The tube with the anode at 70° is the Machlett AEG 50-T, which is ordinarily used to excite characteristic radiation in samples to be analyzed. Usually, this tube is placed so that the radiation passes downward into a box containing the specimen to be analyzed. For our work, the tube is rotated 90° along the tube axis to obtain side discharge, as shown in Fig. II-13.

Another adjustment available in tube position is placement along the tube axis. The tube is moved forward in small steps until the output pattern reaching the crystal position is symmetrical around the crystal axis. This determination may be made by survey with the geiger counter, covered by a mask with a thin slit.

2. Small protractor position

When using a CA-7 tube in the XRD-5 diffraction unit, it is possible to change the angle between the surface of the target and the direction of the beam by rotating the base plate around point A, as shown in Fig. II-14.

The emission intensity pattern of the CA-7 tube is similar to that shown in Fig. II-14. If we need a beam angle of "a" degrees, to fill the width of the soller slit, it is better to obtain the beam at the higher angle so that higher intensity I_2, I'_2, and better distribution are obtained. For our problem the higher angle of the small protractor was always used.

3. Use of soller slits

The XRD-5 is equippped with soller slit collimators in which the plates are stacked one above the other, with each plate parallel to the horizontal plane. As supplied by the manufacturer, the soller slits are designed to minimize vertical dispersion of the beam. Resolution is determined by separate vertical slit systems, which allow for beams with angular spread of 3°, 1°, 0.4°, etc. The small angle slit system transmits a much smaller number of photons, but spatial resolution is high. This system is used with characteristic emission radiation from a CA-7 tube to study, for example, powder diffraction or crystal lattice spacing.

For our problem, the need is to direct a relatively parallel beam of white radiation at an analyzer crystal, and then to accept a relatively monochromatic beam from that crystal to be directed against a target. This latter beam may be fairly large, about 0.5 cm square, but it should be as monochromatic as possible, commensurate with intensity.

It was decided to try soller slit systems to provide the initial parallel beam and also to collimate the monochromatic beam. The soller slit system provides in effect several parallel narrow slits. Medium and high resolution (MR and HR) soller slits were available with dimensions as shown in Fig. II-15.

As indicated previously, provision is made by the manufacturer only for their use with plates horizontal. In our work, they were used with the plates vertical. For test purposes they were fixed to the support, which has positive alignment grooves, with masking tape wrapped around the soller slit cage and the support. The positions occupied by the soller slits and the arrangement used for measuring the energy

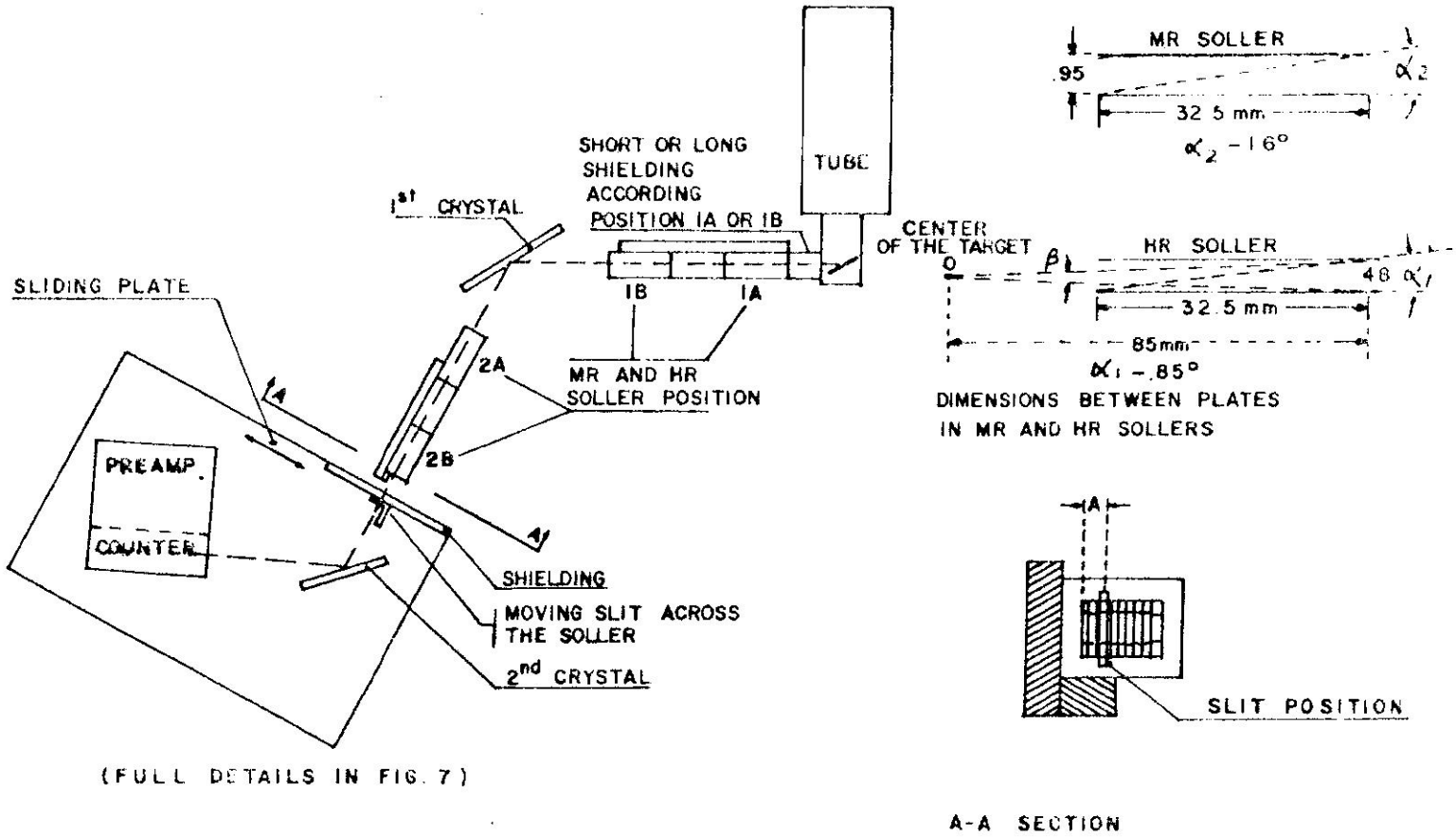

Fig II-15. Soller slit positions

resolution are shown in Fig. II-15.

In each of the arrangements tested, the output from each individual slit of the soller slit system in the number 2 position was measured, obtaining intensity as a function of photoenergy. The results for combination of the High Resolution slit system in position 2B, near the target, and the Medium Resolution slit system in position 1A, near the tube window, are shown in Fig. II-16.

Five different soller slit system arrangements were tested in this way, with the results as shown in Figs. II-17 and II-18. The horizontal straight lines on the energy scale indicate spread between half-peak intensity points.

From these studies, it was apparent that for the different combinations, the total transmitted intensity varied no more than about 2 per cent. However, there were noticeable differences in the photon energy distribution within the beam, with the combination used in Fig. II-16 giving the best results. Geometric analysis likewise predicts that for the soller slit systems we had available, this arrangement would produce the smallest energy spread.

Returning to Fig. II-15, we find that for the HR soller slit system in the 2B position, the dispersion angle is:

$$\tan \beta = \frac{.48}{85} = .00546 \approx \beta \text{ rad.} = .00546 \times \frac{180}{\pi} \approx .3°$$

If we assume that the system is adjusted to accept 7.11 Kev. photons for the extreme (grazing) position, the anticipated wavelength (and energy) spread may be easily estimated.

$$\lambda_1 = 2d \cos (\theta + 0) = 2d \cos (51.2 + 0) = 1.743 \text{ A°} \text{ or } 7.111 \text{ Kev.}$$

$$\lambda_2 = 2d \cos (\theta + \beta) = 2d \cos (51.20 + 0.3) = 1.743 \times \frac{.62251}{.62660} =$$

$$= 1.732 \text{ A°} \text{ or } 7.157 \text{ Kev.}$$

The anticipated spread is thus about ± 46 e.v. The experimental results in Fig. II-16 show no more than 90 e.v. spread to half maximum for any one slit.

Finally, for the case in Fig. II-16, the energy distribution for the whole beam was obtained by graphical integration. The beam intensity as a function of photon energy is represented in Fig. II-19a. This is the result for one slit. In Fig. II-19b, the beam intensity as a function of its position in the beam cross section is shown. Combining the information in these curves for each measurement position in the beam cross section, we obtain Fig. II-20, the energy distribution of the photons in the whole beam. The energy resolution is quite good. The spread to the half intensity point is only ± 35 e.v. Within ± 50 e.v., 81.6 per cent of all the energy is found. Thus, meaningful irradiation tests at intervals of 100 e.v. can be carried out.

The interval between the K α_1 emission lines for elements around iron is about 500 e.v. This is important in comparing the use of the "monochromatic" radiation available from a crystal diffraction unit with that available by use of fluorescence emission. The closest emission line to the K absorption edge of iron at 7.111 Kev is the cobalt Kα_1 line at 6.930 Kev. If the effect being sought has a strong dependence on energy, and is associated with the absorption edge, it could easily be missed if only fluorescence radiation were used.

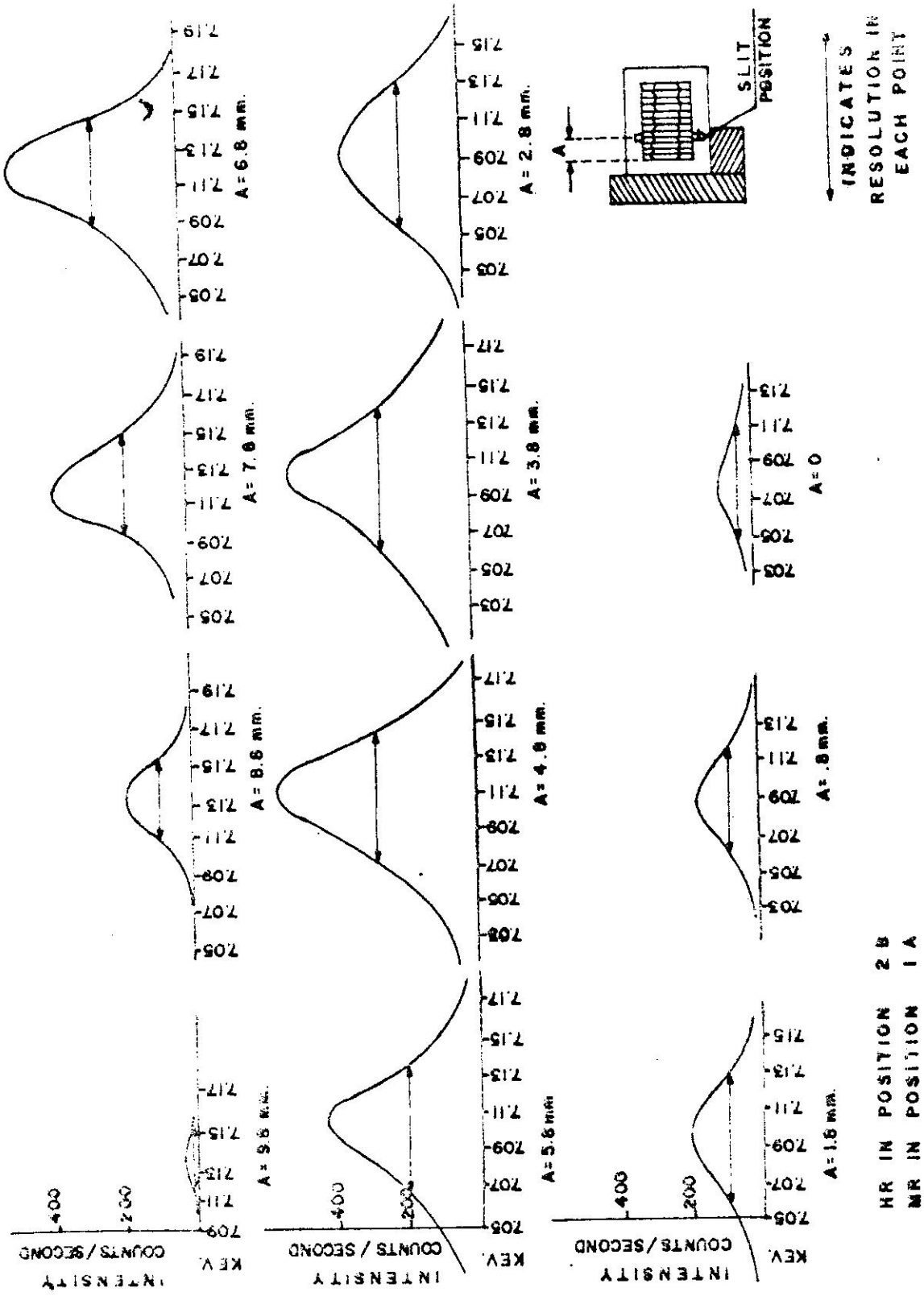

Fig. II-16. Energy distribution in different points across the beam

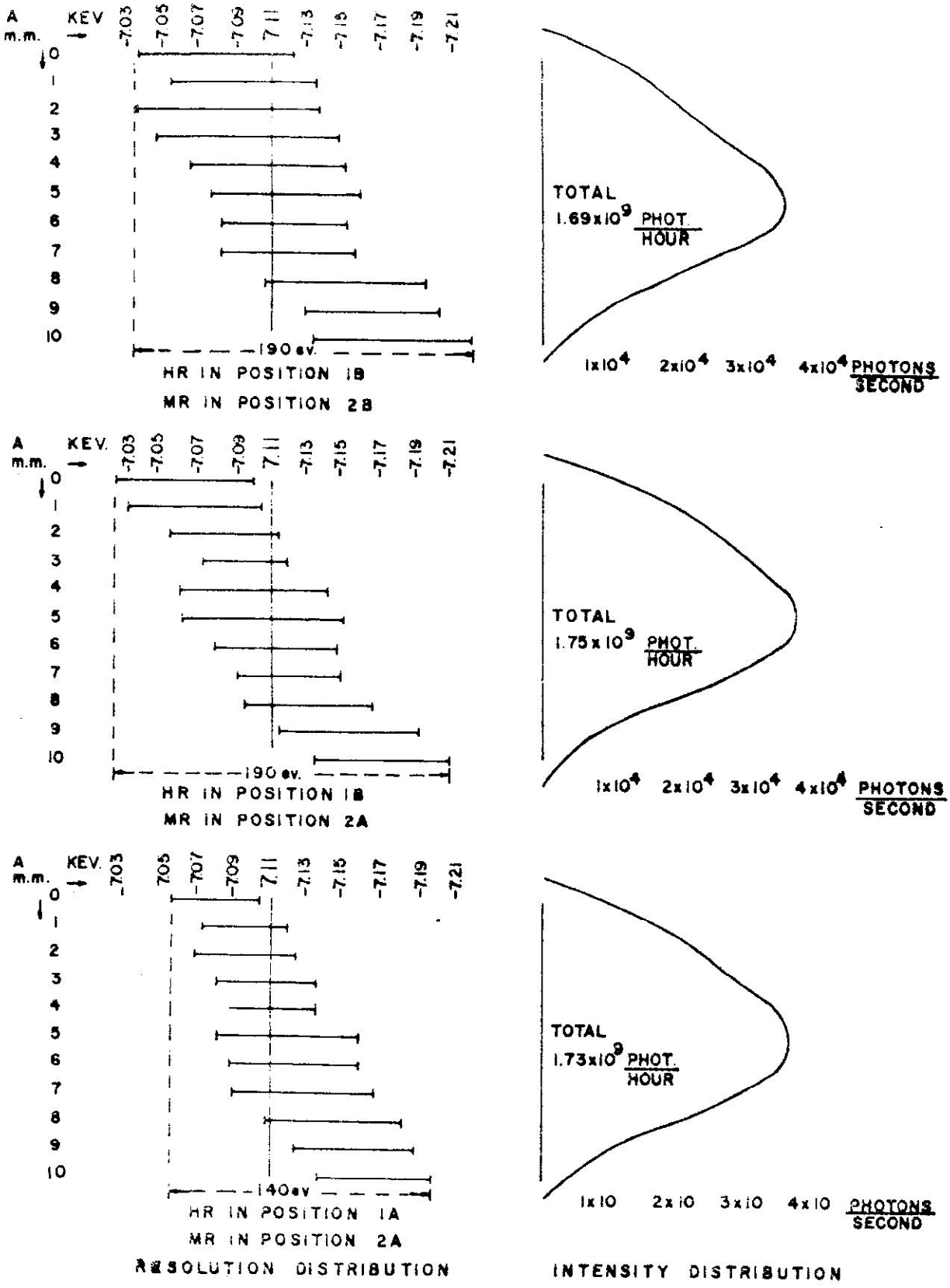

Fig. II-17. Resolution and intensity distribution across the beam

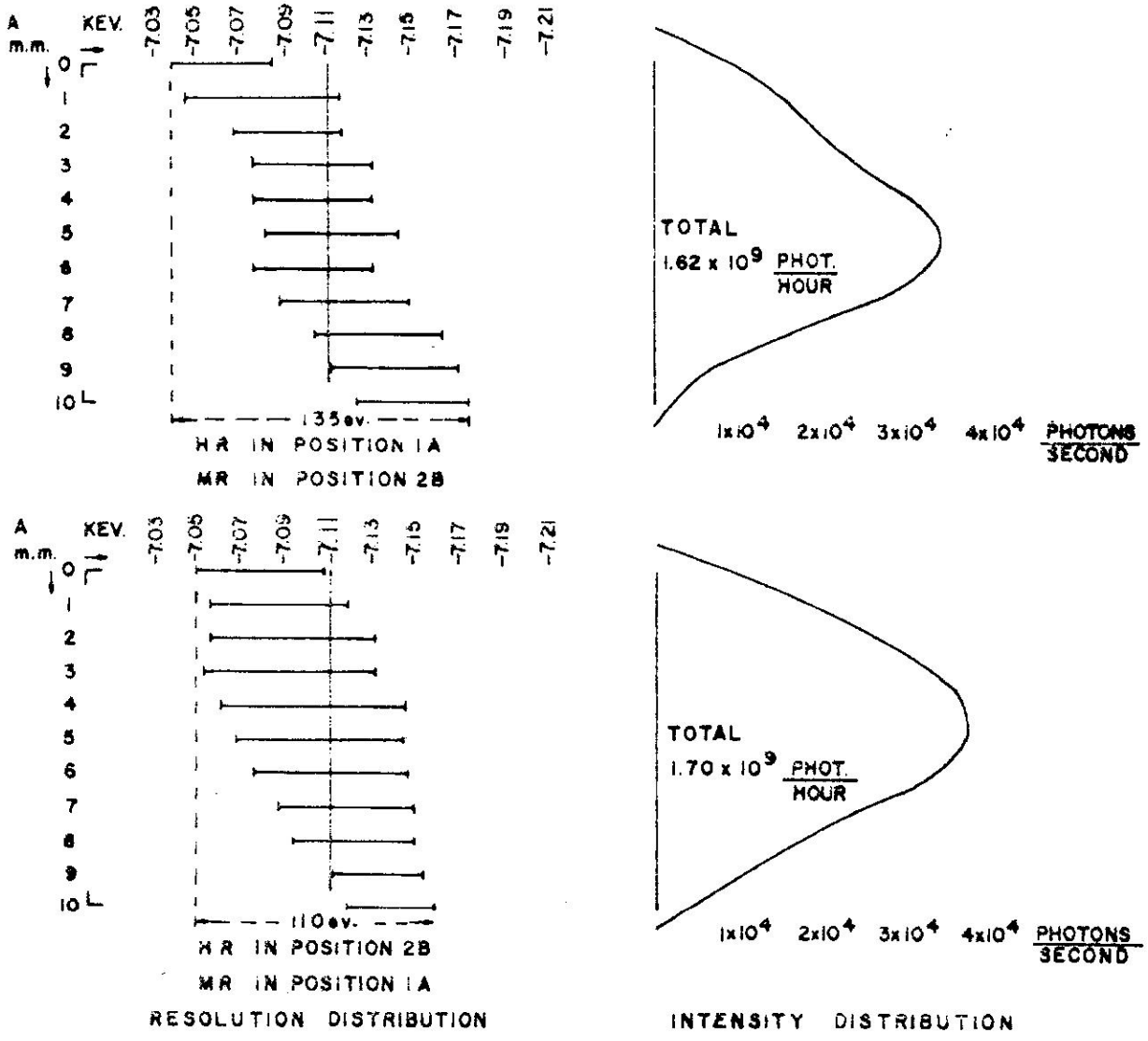

RESOLUTION DISTRIBUTION

INTENSITY DISTRIBUTION

NOTE: 1-A THE SAME AS IN FIGURE 16

Fig. II-18. Resolution and intensity distribution across the beam

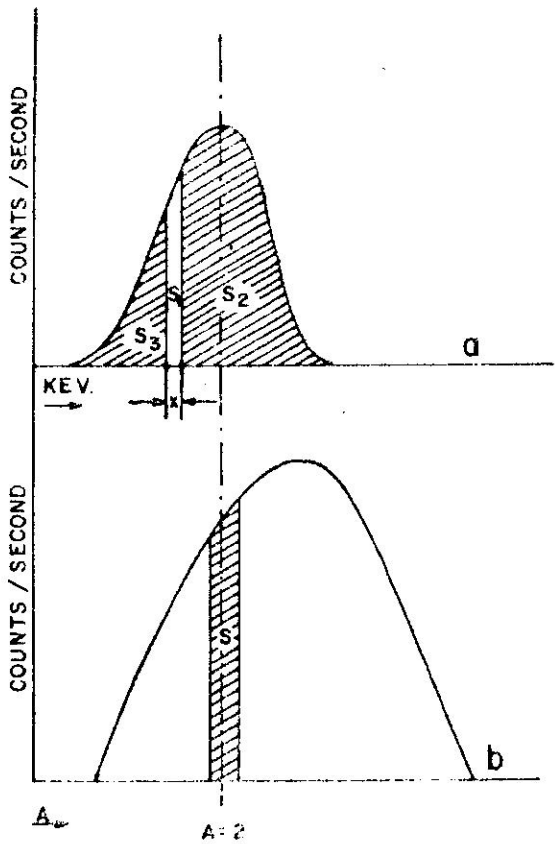

Fig. II-19. Total intensity distribution across the beam and energy distribution at point A - 2

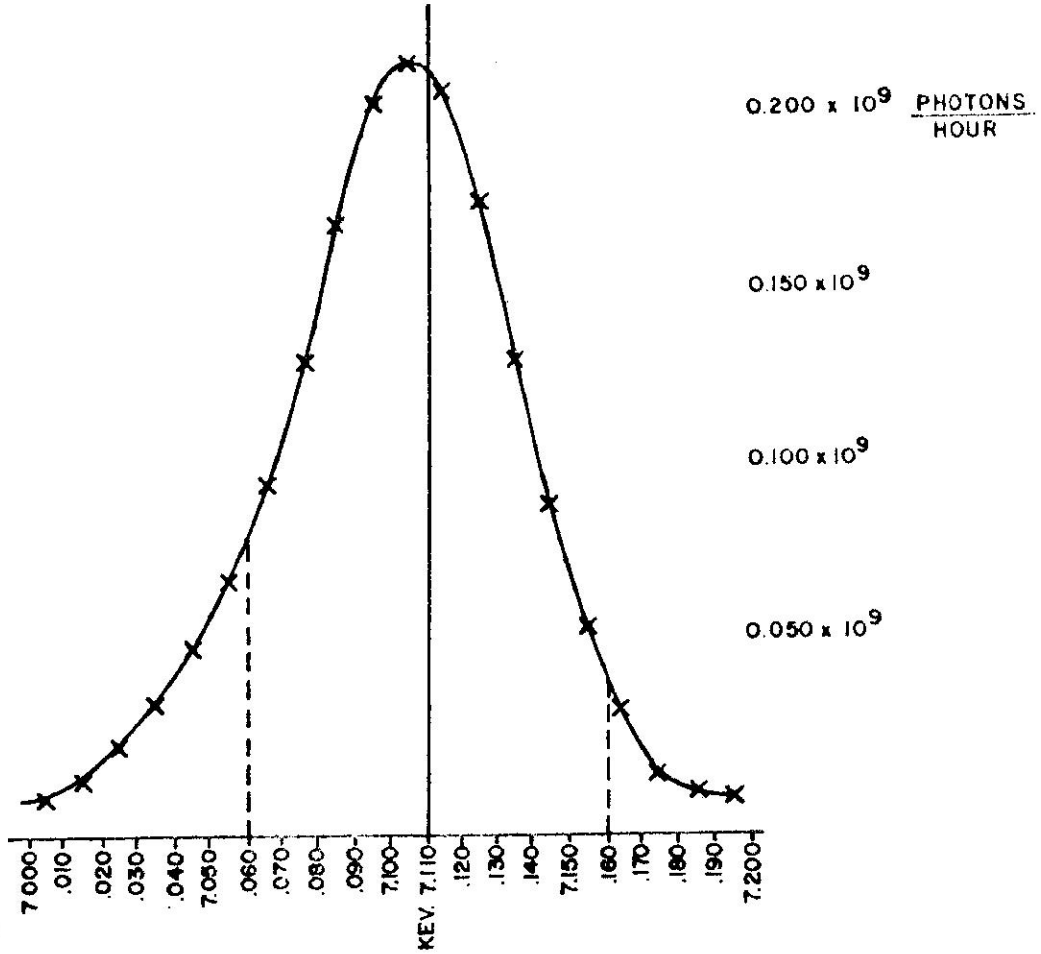

Fig. II-20. Energy distribution of photons in the whole beam

H. LITERATURE REFERENCES

1. Clendinning, W. R. and Atkins, M. C. Methods of Monochromatic Irradiations and Absolute Dosimetry with Soft X-Rays. Resonance in Radiation Effects Report No. 3, The University of Michigan, Ann Arbor, (1960).

2. Compton, A. H. and Allison, S. K. X-Rays in Theory and Experiment. New York: Van Nostrand Company, Inc., (1935).

3. Emmons, A. H. Resonance Radiation Effects of Low Energy X-Rays on Catalase. Ph.D. Thesis, The University of Michigan, Ann Arbor, (1959).

4. Clark, G. L. Applied X-Rays. New York: McGraw-Hill Book Co., (1955).

5. Meyer, Charles F. The Diffraction of Light, X-Rays, and Material Particles. J. W. Edwards, Ann Arbor, Michigan, (1949).

6. Advances in Spectroscopy. Edited by H. W. Thompson, Vol. I. Interscience Publishers Inc.

7. Peiser, H. S., Rooksby, H. P., Wilson, A. J. C., Ed. X-Ray Diffraction by Policrystaline Materials. Chapman and Hall Limited, Reinhold Publishing Corporation, New York, (1960).

8. James, R. W. The Crystalline State. Vol. II, G. Bell and Sons Ltd. (1955).

9. Klug, Harold P., Alexander, Leroy E. X-Ray Diffraction Procedures. John Wiley and Sons, Inc. New York, Chapman and Hall, Ltd. London, (1954).

LIST OF FIGURES

I-1. Resonance radiation effects on catalase - data of Emmons 5

I-2. Resonance radiation effects on catalase - data of Paraskevoudakis 5

I-3. Sketch of sample holder 6

I-4. Comparison of sensitivity of various methods for determining ferric ion in dosimeter..... 9

I-5. Monochromatic x-ray beam intensity as function of photon energy 15

I-6. Resonance radiation effect of monochromatic x-rays on catalase 18

I-7. Comparison of absorbance and percent transmission plots vs. enzyme concentration 28

I-8. Apparent velocity constant vs. enzyme concentration (simplified data)..... 29

II-1. Photograph of General Electric X-ray diffraction unit XRD-5 38

II-2. X-ray emission distribution 39

II-3. Crystal length 42

II-4. Photograph of the diffraction unit with counter on sliding device 46

II-5. Sliding device sketch 47

II-6. Intensity distribution 48

II-7. Photograph of diffraction unit with double diffraction device 50

II-8. Double diffraction device 51

II-9. Target emission patterns 54

II-10. Component orientation for second harmonic studies (absorption method) 57

II-11. Component orientation for second harmonic studies (double diffraction method) 57

II-12. Percentage of second harmonic contamination 59

II-13. Tube and diffraction unit with small protractor ... 60

II-14. Target angular intensity distribution 63

II-15. Soller slit positions 66

II-16. Energy distribution in different points across the beam 69

II-17. Resolution and intensity distribution across the beam 70

II-18. Resolution and intensity distribution across the beam 71

II-19. Total intensity distribution across the beam and energy distribution at point A = 2 72

II-20. Energy distribution of photons in the whole beam .. 72